UNIVERSITÄTSKLINIKUM HAMBURG-EPPENDORF

Zentrum für Psychosoziale Medizin
Klinik für Psychiatrie und Psychotherapie
Arbeitsgruppe Bildgebung

Direktor: Prof. Dr. Jürgen Gallinat

The Interhemispheric Coupling of Auditory Cortices

Dissertation

zur Erlangung des Grades eines Doktors in der Medizin
an der Medizinischen Fakultät der Universität Hamburg.

Vorgelegt von:

Rom Amselberg
aus Petach Tikva, Israel

Hamburg 2019

1. **Gutachter:** Prof. Dr. Christoph Mulert

2. **Gutachter:** Dr. Michael Hauck

Datum der Disputation: 06.02.2019

Table of Contents

Disclaimer

Partial results of the presented work have been published in:

Steinmann S, Amselberg R, Cheng B, Thomalla G, Engel A K, Leicht G and Mulert C. The role of functional and structural interhemispheric auditory connectivity for language lateralization - A combined EEG and DTI study. Sci Rep. 2018;8(1):15428. Published 2018 Oct 18. doi:10.1038/s41598-018-33586-6

The figures 4, 12, 19 and 20 with the corresponding legends were previously published in the aforementioned article. Experimental results of the article were obtained in parallel to completing this doctoral thesis. Scientific Reports does not require authors to assign copyright of their published original research and allows re-use.

1. Introduction

Theoretical advances in language research and the availability of high-resolution neuroimaging techniques in the neurosciences profoundly improved the investigation of the neurophysiological mechanism of speech and language processing. Despite significant progress, the understanding of language and speech processing is still far from sufficient. Recent studies closely aligns language research with issues at the core of systems neuroscience, ranging from neurophysiological and neuroanatomic characterisations to questions about neural coding.

One big questions, with regard to speech and language processing in neuroscience, concerns “lateralisation of function” and “hemispheric dominance”. Among right-handed people the contralateral left hemisphere (LH) is dominant for speech and language processing. The classical concept of brain and language was formed in the 19th century, describing areas such as Wernicke centre, as sensory speech centre, and Broca as motor speech centre. The current point of view posits that many bilateral brain structures interact in vast neuronal networks for the matter of speech and language processing. Our current understanding rejects the classical concept of certain functions being executed by certain areas of the brain. Many such concepts rely on deficit-lesion correlations observed in stroke patients more than a hundred years ago. For example, new evidence show that a Broca area lesion does not always lead to a Broca's aphasia. Accordingly, a Broca's aphasia does not always result from a Broca area lesion. However, in clinical contexts, these classical concepts developed more than a 100 years ago still dominate (Poeppel et al. 2012).

Thus, interhemispheric interaction is crucial for healthy language processing and comprehension. The dichotic listening (DL) paradigm is a perfect paradigm to investigate auditory perception and interhemispheric interaction. It is often used to determine hemispheric laterality and asymmetry .

1.1 Working hypothesis and aims

Accordingly, the present thesis deal with the role of the structural and functional interhemispheric connectivity in normal auditory perception. The aim was, in

particular, to examine the association between speech lateralisation (measured with the DL task) and functional connectivity in the gamma-band range (derived from EEG recording conducted during DL task), as well as with the structural white matter (WM) DTI information. It was hypothesised that there is a close relation between functional as well as structural interhemispheric auditory connectivity and conscious auditory perception during DL. This thesis first provides a short theoretical background on the current state of knowledge regarding auditory processing, the DL paradigm and applied neuroimaging methods (chapter 1). The main part of the thesis describes the performed study with its methods and material (chapter 2), its results (chapter 3) and its discussion (chapter 4). Finally, a concise summary of the thesis is given (chapter 5).

1.2 Auditory processing

The auditory pathway is illustrated in Fig. 1 (modified after Trepel 2015). It begins in the inner ear (1 in Fig. 1) with the afferent fibres of first neurones, which are bipolar neurones. These neurones are located in the spiral ganglion and transfer their potentials to the cochlear nuclei (2) in the medulla oblongata. The fibers continue here through either (mostly) the corpus trapezoideum (3), or through the nucleus olivaris superior (4) and cross to the contralateral side. A few other fibres doesn't cross through the corpus trapezoideum and continue upwards ipsilateral and enter the colliculus inferior. Fibres that have went through the nucleus olivaris superior switch there to the third neuron. This switch to the third neuron is relevant for directional hearing. All fibres that have crossed to the contralateral continue as the lateral lemniscus (5) to the colliculus inferior (7). A few fibres switch once again in the nucleus lemnisci lateralis (6). Some of these cross here back to the ipsilateral towards the parallel nucleus lemnisci lateralis and continue from there to the colliculus inferior, where they meet the fibres which didn't cross in first place and continued ipsilateral upwards, others return to the lateral lemniscus (5). Some fibres cross from one inferior colliculus to the contralateral, while most of the fibres continue via the brachium of the inferior colliculus to the medial geniculate body (8) of the thalamus. The fibres are switched the medial geniculate body once again and continue to the transverse temporal gyrus, also known as Heschl's gyrus (HG), Brodmann area 41 or as the primary auditory cortex (PAC) (10). The entire auditory pathway is organised in a tonotopic arrangement, meaning the fibres and neurones

are organised spatially by sound frequency. This enables differentiation of high and low sounds. Within HG, fibres of deep sounds (low frequency) terminate anterolateral while those of high sounds terminate posteromedially. Moreover, some fibres of the lateral lemniscus cross back to the ipsilateral side, meaning that each PAC receive auditory input from both ears .

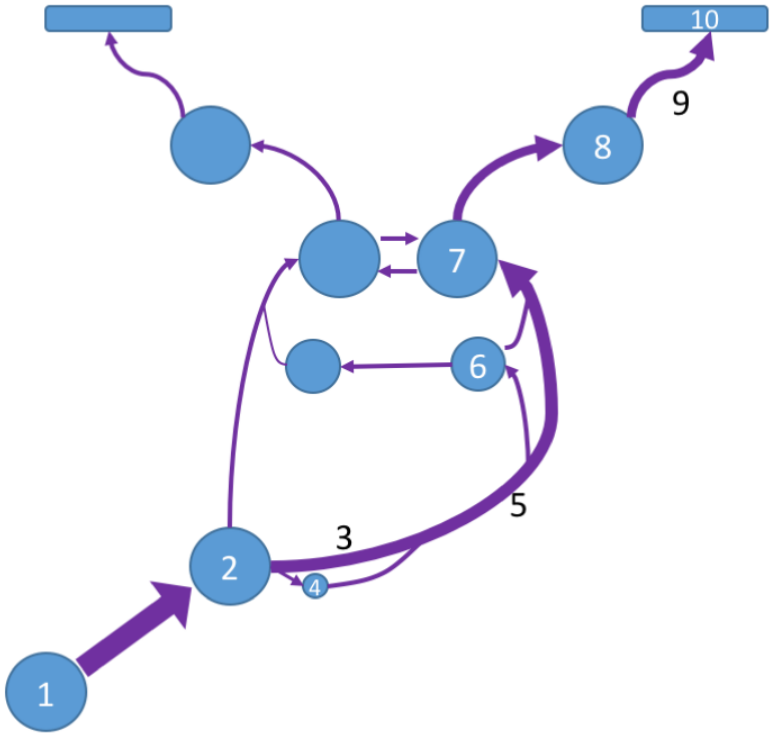

Fig. 1. **1**. cochlea, **2**. nucleus cochlearis, **3**. corpus trapezoideum, **4**. nucleus olivaris superior, **5**. lateral lemniscus, **6**. nucleus lemnisci lateralis, **7**. colliculus inferior, **8**. medial geniculate body, **9**. acoustic radiation, **10**. PAC.

Similarly to the area striata or the postcentral gyrus, as primary visual and somatosensory cortices, HG is responsible for auditory perception of tones with no further interpretation. The interpretation of sounds into melodies or words happens in the secondary auditory cortex (SAC). Efferents from HG terminate at the SAC. The SAC consists of Brodmann areas (BA) 42 and 22 and lies directly next to the PAC. In the SAC, auditory impulses become words, sounds and melodies (Trepel 2015). According to studies by Boatman (2004) and Hickok and Poeppel (2007) the posterior division of the superior temporal gyrus (pSTG) is critical for acoustic-phonetic processing. This area corresponds approximately to BA42. The SAC has different functions in each hemisphere. The one in the dominant hemisphere, usually the LH among right-handed people, is known as the sensory speech centre

or as Wernicke centre and is responsible for the rational understanding of language. The SAC in the non-dominant hemisphere is responsible for less rational aural evaluation such as understanding music. Wernicke centre is relevant not only for heard and spoken language, but also, and perhaps more relevantly, for thinking, which is usually a verbal process (Trepel 2015).

1.3 Dichotic Listening (DL) task and interhemispheric auditory connectivity

Dichotic listening (DL), from Greek **διχο-** *dikho-* apart and οὖς, *ous*, *ot-* ear, describes the process of presenting two different sounds simultaneously to the right (RE) and the left ears (LE) (Oxford 2015). DL was first demonstrated by Broadbent (1954) in the form of a test using earphones and was later modified by Kimura (1961a, 1961b). Kimura observed during DL more correct reports from the RE than from the LE – an effect that was described as superior effectiveness of the connections of each ear to the contralateral hemisphere over ipsilateral connections, as well as a tendency towards a right ear advantage (REA) (1967). She explained the REA finding in DL tests might be due to a better and shorter connection of the RE to the LH, as well as the assumption that the LH is where speech sounds are analysed. Therefore inputs to the LE first enter the right hemisphere (RH) and require further interhemispheric transfer to the LH. The WM links between both left and right auditory cortices connect tonotopically organised subregions for different sound frequencies (Lee and Winer 2008). Verbal input from the RH needs to be transferred via the callosal body (CC) to the LH for further processing (Hugdahl et al. 1997). Since the LH is most important for language and since contralateral pathways appear to be more dominant within binaural perception, it is assumed that the callosal pathway is the most important one for hearing (Bamiou et al. 2007). It have been shown that these intrahemispheric connections between left and right auditory cortices go through the isthmus and splenium of the CC located in its posterior third (Aboitiz et al. 1992), the pathways are schematically visualised in Fig. 2 (Steinmann et al. 2014a).

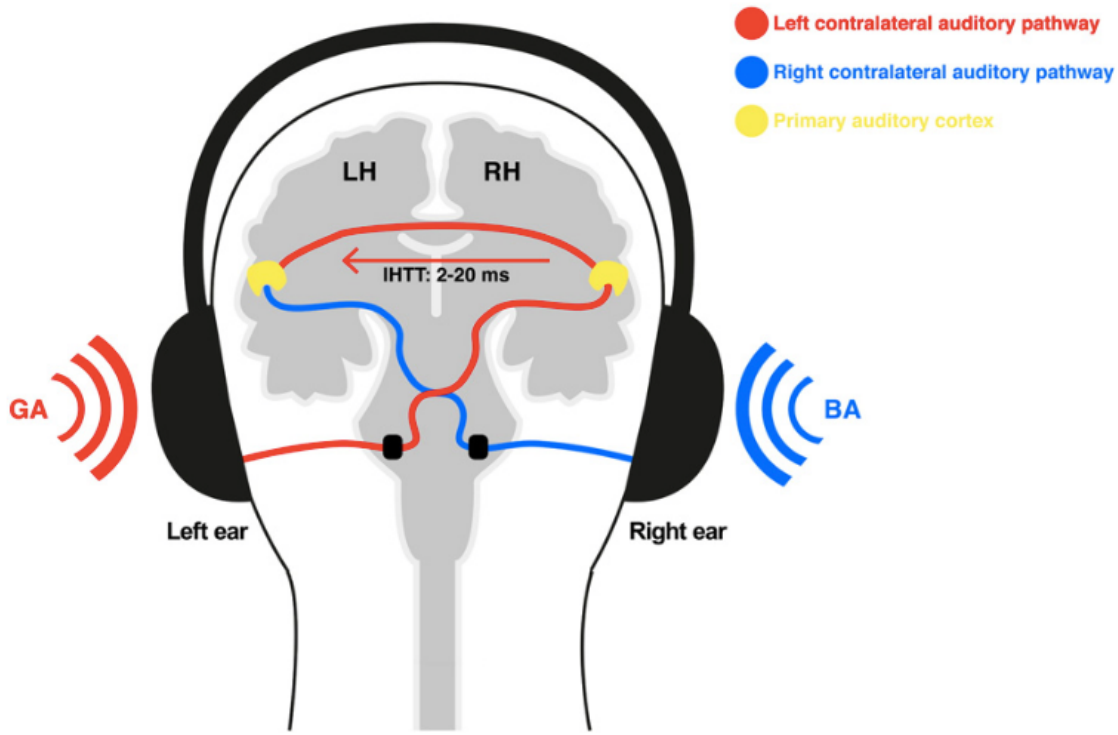

Fig. 2. Two syllables are presented at once. One (ga) to the LE, the other (ba) to the RE. Despite the existence of ipsilateral pathways, the contralateral ones appear to be superior (Kimura 1967) and it is even assumed that the ipsilateral pathways are blocked during DL (Brancucci et al. 2004). The contralateral pathway, connecting the RE directly with the LH is illustrated by the blue line whereas the red lines indicate the indirect pathway from the LE, initially to the RH and then across the CC to the LH. LH: Left hemisphere, RH: Right hemisphere, IHTT: Interhemispheric transfer time (Henshall et al. 2012).

The DL task is the most commonly used paradigm to investigate the relation between interhemispheric interaction, conscious auditory perception, and language lateralisation (Westerhausen et al. 2009). In particular, understanding the neurophysiological underpinning of those three parameters within healthy probands plays a crucial role for the investigation of different patient groups, such as schizophrenia patients who suffer from auditory verbal hallucinations (AVH) (i.e. hearing voices), or patients with tinnitus (i.e. auditory phantom precept) that show alterations in this regard. It has been shown in a meta-analysis of DL studies (Ocklenburg et al. 2013) that reduced left-hemispheric language lateralisation correlates strongly with the occurrence of AVH in patients with schizophrenia (see review by Steinmann et al. 2014b). In addition, Diesch et al. (2012) showed an alteration of CC size and auditory cortex volume within patients suffering from tinnitus compared to healthy controls.

The DL task is often combined with neuroimaging procedures such as EEG, DTI, magnet resonance imaging (MRI) or functional MRI (fMRI) in order to acquire more

information about the underlying pathophysiological mechanism. In many of these cases, both test and imaging procedures occur at once, while simultaneous procedures involving an MRI scanner (DTI, MRI, fMRI) have the disadvantage of the scanner noise interfering with the perception of sound affecting the results of the DL task (Dos Santos Sequeira et al. 2010). The combination of EEG and DL task is probably the most insensitive to such influences since EEG is usually conducted in an environment with no background noise. While DL task only produces behavioural information about the proband, it usage in combination with EEG offers information such as [1] auditory-evoced potentials visible in each hemisphere, [2] involved cortical regions, and [3] synchronisation of regions with its different patterns appearing while choosing left or right input. The interhemispheric pathways linking both auditory cortices go mostly through the CC. DTI is therefore a good neuroimaging method to visualise and study this connection. DTI provides information on the structural connectivity of selected regions of interest (ROI), which are in this case HG and pSTG. It can show the connection itself as well as supply information on the fibres integrity such as the fractional anisotropy (FA). FA provides information about the micro architecture of WM, which adds another dimension to understanding of language lateralisation and interhemispheric connectivity.

In summery, EEG can provide high temporal resolution, while DTI and MRI provide high structural and spatial resolution. The combined usage of both methods allows for new opportunities, bigger than those of each method on its own. It allows for a better understanding of physiology and of pathophysiology. A study combining DTI and DL task conducted by Ocklenburg et al. (2014) showed that both FA and volume of the left arcuate fasciculus correlates positively with REA. This finding affirms the notion, that the micro- and macro structural properties of the brain and behavioural traits are associated. Another study combining EEG and DL task by Steinmann et al. (2014) showed that interhemispheric lagged phase synchronisation (LPS) of gamma-band oscillations (GBO) between left and right auditory cortices was increased for LE reports. Increased LPS can be interpreted as stronger interhemispheric information transfer between auditory cortices. Moreover, it was shown that subjects are likelier to report RE inputs when interhemispheric connectivity is lower. These findings suggest that during conscious perception of LE reports the interhemispheric gamma-band connectivity between bilateral auditory

cortices is increased and that the size of underlying fibre tract correlates positively with the number of LE reports (Westerhausen et al 2009).

1.4 Electroencephalography (EEG)

Electroencephalography (EEG, from Greek ἐγκέφαλος enképhalos “brain” and γραφία graphia “writing”) is the noninvasive registration of the electric activity of the brain by creating a graph illustrating the change of potential difference over time, as measured by electrodes attached to the head. While measured at the scalp, the signal actually originates from pyramidal neurones of the cortex. The sum of synchronised postsynaptic potentials of thousands of pyramidal neurones creates a scalp potential. These potentials are a result of a complex network of neurones of the cortex and of deeper structures such as the thalamus (Alvarez and Rossetti 2014).

The first one to register cortex potentials was Richard Caton. Caton examined the brains of monkey and rabbit, using two electrodes placed on the cortex or on the skull, over which he measured potential differences. He noticed that the electric activity of the grey matter is related to its function (Caton 1875). In the nineteen-twenties Hans Berger succeeded in recording a human EEG registering the electric activity at the scalp (Berger 1929). Therefore Hans Berger is considered to be the inventor of EEG.

Using EEG it is possible to investigate the state of consciousness and cognitive activity. There are many applications of EEG in clinical routine, among these: to diagnose Epilepsy in the neurology, to identify sleep phases in the somnology, to determine cerebral death, to monitor narcosis depth (BIS) and avoid awareness in operations in the anesthesiology or to monitor coma in the ICU. It can be interpreted longitudinally, i.e. the same way as a conductor reads the sheet music of a symphony, or it can be computer analysed, e.g. by averaging many EEG signals recorded after a repeated event for each electrode, searching for correlations between electrodes or analysing by frequency or amplitude spectrum (Zschocke and Hansen 2012).

The EEG is typically described in terms of bands, mostly in four wave patterns according to their frequency (in Herz, Hz). Alpha (α, see fig. 3.) is the frequency range from 8 to 13 Hz and emerges while the proband is relaxed with closed eyes. Beta (β) is the frequency range from 13 to 30 Hz. Beta is typical for cognitive activity and concentration and also replaces the alpha waves upon eyes opening, a phenomenon also known as alpha-block or the Berger-Effect (after Hans Berger). Theta (θ) is the frequency range from 4 to 8 Hz, while delta (δ) ranges in frequency range from 0.5 to 4 Hz. Both frequencies emerge in somnolence and in some states of sleep. It appears that different regions of the brain tend to produce distinctive rhythms. For example, theta waves are more common in temporolimbic regions (Zschocke and Hansen 2012).

Another fast rhythm is the gamma-band (γ) rhythm with a frequency range from 30 to 100 Hz. It is typical for high attention for conscious perception, when vast nets of widely distributed neurones are functionally connected. Different types of neurones in different regions of the cortex can be connected to a group by means of activity synchronisation in 30 to 100 Hz frequency which makes them into an ensemble. The role of GBO was mostly examined in relation to the visual system, and therefore less is known about its role in the auditory modality (Pape 2014, Steinmann et al. 2014a). Several studies have shown that functional connectivity in the gamma-band, i.e. synchronizsation of GBO between local and/or distant neurones are associated with cognitive or perceptual processing: in a 2008 conducted EEG study using gamma-band phase synchronisation it was shown that synchronisation of GBO between inferior and medial temporal regions was crucial for working memory (Axmacher et al, 2008). Moreover, it appears that anatomical connectivity, i.e. WM connections, is more important than topographic proximity, considering the strength of oscillation synchrony in the gamma-band range (Csicsvari et al. 2003, Mulert et al. 2011).

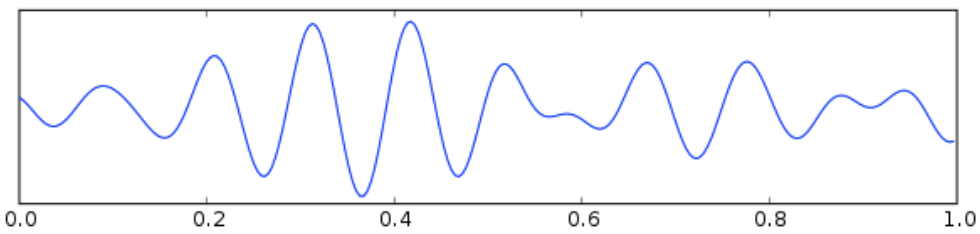

a. Alpha waves

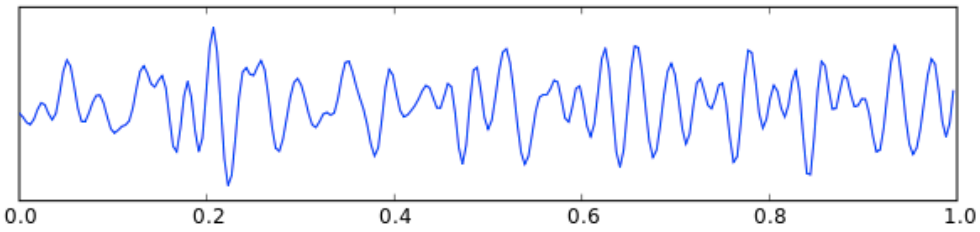

b. Beta waves

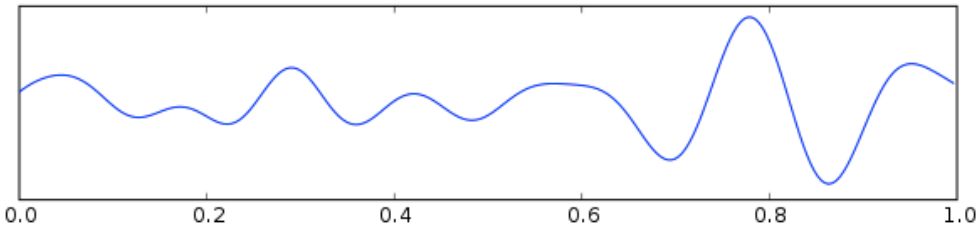

c. Theta waves

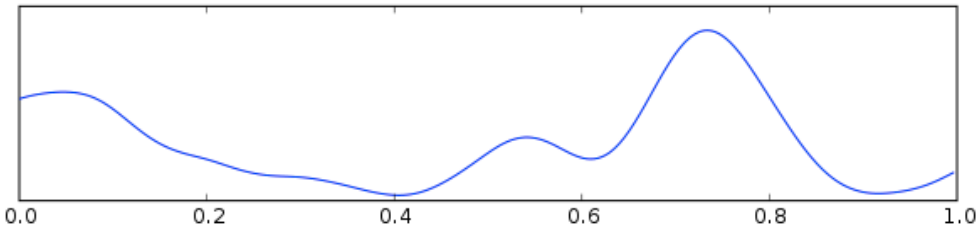

d. Delta waves

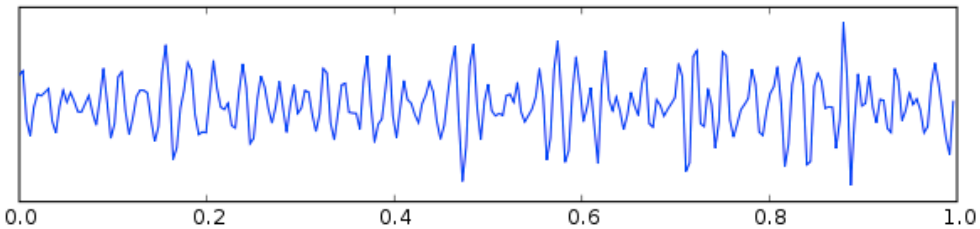

e. Gamma waves

Fig. 3 a - e. All images are free medias from Wikimedia, created by Hugo Gamboa.

One analytic parameter of functional connectivity is the LPS (Pascual-Marqui 2007a). It describes the similarity of oscillation within a defined spectrum of frequencies between two signals based on normalised (unit module) Fourier transformation, and hence is parallel to nonlinear connectivity. The measured value correlates with the connectivity of the two signals. The calculation of the LPS takes the zero-lag contribution into account and excludes it. In a defined frequency spectrum, Zero-lag connectivity, unlike nonzero-lag connectivity is in many occasions a result of artefacts created by non-physiological effects. Zero-lag contribution to signal might therefore function as a confounding factor. LPS, which is clean of zero-lag contribution, virtually contains only physiological effects (Stam et al. 2007, Steinmann et al. 2014a).

Classical phase synchronisation is by definition:

$$\varphi^2_{x,y}(t,\omega) = \left|f_{x,y}(t,\omega)\right|^2 = \left\{\mathrm{Re}\left[f_{x,y}(t,\omega)\right]\right\}^2 + \left\{\mathrm{Im}\left[f_{x,y}(t,\omega)\right]\right\}^2$$

with:

$$f_{x,y}(t,\omega) = \frac{1}{N_R}\sum_{k=1}^{N_R}\left[\frac{x_k(t,\omega)}{|x_k(t,\omega)|}\right]\left[\frac{y^*_k(t,\omega)}{|y_k(t,\omega)|}\right]$$

xk (t, ω) and yk (t, ω) express the discrete Fourier transform of both signals for the k EEG period (1 to NR), t is time, ω is frequency. * describes complex conjugate. This definition is problematic since it is highly influenced by artefacts and components that might be attributed to non-physiological effects. The LPS removes the instantaneous artefactual components and is defined as:

$$\varphi^2_{x\rightleftharpoons y}(t,\omega) = \frac{\left\{\mathrm{Im}\left[f_{x,y}(t,\omega)\right]\right\}^2}{1-\left\{\mathrm{Re}\left[f_{x,y}(t,\omega)\right]\right\}^2}.$$

(Stam et al. 2007, Steinmann et al. 2014a)

Steinmann et al. (2014) examined using EEG the LPS between bilateral auditory cortices in reference to DL. As postulated, LPS was increased within probands who reported more LE presentations. As described above, within normal population the REA is the typical configuration (Hugdahl et al. 1997). Since an increased LPS is interpreted as higher connectivity, it has been assumed that a tendency to report more LE inputs is due to an improved information transfer between both auditory cortices.

1.5 Diffusion Tensor Imaging (DTI)

Diffusion tensor imaging, also known as diffusion tensor magnetic resonance imaging (DT-MRI), is a noninvasive imaging technique, developed in the early 1990s. Water molecules move randomly in space in all directions equally (Brownian Motion). Unrestricted diffusing water molecules would therefore move in all directions equally, thus in a gradually growing spherical shape. This is defined as isotropic diffusion. In vivo, water diffusion pattern is modified by the organised architecture of the biological tissue. For example, diffusion in axons is hindered by myelin sheaths, cell membranes and micro filaments. The result is a tendency of

water molecules to move in some directions more than in others. This pattern is described as anisotropic diffusion. Since the WM of the brain is organised in parallel fibres (axons) covered with myelin sheaths, water diffusion within the WM is highly anisotropic, i.e. the water molecules mobility in WM is not the same in all directions (Le Bihan 2003, Koerte and Muehlmann 2014).

The DTI technique relies on the anisotropic diffusion property of water molecules in the brain parenchyma, providing information about the fine architecture of brain tissue such as direction and density of fibres. An MRI scanner adjusted to produce a DTI image uses a sequence of radio frequency pulses and magnetic gradients to create a single measurement. As a result, for each such measurement, a three-dimensional volume is created in which every voxel (volumetric element) has a value proportional to the diffusion component parallel to the gradient direction. Three such measurements are required to determine the rate of diffusion in each voxel. Six measurements are required to create a tensor, containing not only the rate of diffusion of each voxel but also its directionality. A diffusion tensor is often regarded as a 4D volume, and can be visualised as an ellipsoid with three eigenvalues and three eigenvectors at every voxel. The eigenvalues represent the length of the axis of the ellipsoid. The eigenvectors represent the orientation of each axis. The length is proportional to the rate of diffusion parallel to the axis. The first eigenvalue, L1 is the main axis of the ellipsoid: the longest one. L2 is the longest orthogonal one to it and L3 is orthogonal to both axes.

Interestingly, studies combining DTI and EEG techniques have been conducted to improve the understanding of the structure-function relationship (Finger et al. 2016). A very recent EEG-DTI study examined the FA-value of the cingulum and of CC related fibres, as well as theta and alpha band activity (qEEG of several cortical and subcortical structures) of thalamic stroke patients, and found correlations between FA and the power of the alpha / theta activity (Duru et al. 2016). Another study on patients suffering from Alzheimer's disease found an association between reduced FA within the CC and a reduced functional connectivity between all major cortical areas of both hemispheres (i.e. by means of increased delta and decreased alpha period duration). This finding indicates that decreased functional connectivity can be used as a marker for degeneration, and therefore reduction of fibres connecting both hemispheres (Vecchio et al. 2015).

2. Materials and methods

2.1 Participants

Participants were 30 healthy right-handed individuals (15 male) aged 20-50 years who were recruited through postings on university recruitment sites and local media. Exclusion criteria were actual or former neurological or psychiatric disorder, left-handedness, diagnosis of schizophrenia in second degree relative or higher, a hearing impairment or notable medical condition, and an intelligence quotient below 70. Furthermore, we excluded subjects with metal implants made of ferromagnetic metal or those sensitive to magnetic fields and subjects who suffer from claustrophobia. Handedness was estimated with the Edinburgh Handedness Inventory (Oldfield 1971). To warrant hearing is normal in both ears, subjects were examined by a hearing test for frequencies between 120 and 8000 Hz (Esser Home Audiometer 2.0). Participants who had an auditive threshold of 25 dB or higher, or those with an interaural discrepancy of 15 dB or higher in one or more of the examined frequencies were ruled out of the study. Participants who were bilingual or multi-lingual at native speaker level, as well as ambidextrous had to be excluded. This study was approved by the ethics commission of the Medical Association Hamburg. All practiced methods were conform with all important regulations and guidelines. All subjects were informed about the specifics of the experiment and signed an informed consent document complying with the Decleration of Helsinki. Demographics regarding all participants are shown in Table 1.

Table 1: Demographic characteristics, DL and DTI results. SD: standard deviation. Mean: arithmetic mean.

	All Subjects (n=27)		
	Mean	SD	Range
Age (years)	30.19	8.54	20-50
Sex (male:female)	14:13		
Handedness	90.62	13.89	40-100
Education (years)	17	1.93	13-21
RE reports	134.04	28.29	85-184
LE reports	81.26	17.18	50-112
Error reports	24.81	15.42	2-55
Laterality Index (LI)	23.56	19.7	(-11)-57
Vocabulary test (IQ)	109.96	8.84	86-133
FA of HG	0.45	0.027	0.38-0.49
FA of pSTG	0.44	0.02	0.41-0.49
LPS of HG	0.0105	0.0021	0.01-0.02
LPS of pSTG	0.44	0.02	0.41-0.49

The experiment was conducted in two separate and randomized sessions (EEG and DTI) at the University Medical Center of Hamburg and consisted of following parts: a psychiatric questionaire, a sociodemographic questionaire, Edinburgh Handedness Inventory (Oldfield 1971), a standardised German vocabulary test (Herzfeld 1994), a hearing test (Esser Home Audiometer 2.0), 64 channel EEG (4 of originally 64 electrodes were used to track eye movement) measurement consisting of a standardised routine EEG and two blocks of DL task and a MRI scan consisting of a short spatial orientation scan, a T1 weighted sequence and a DTI sequence in 60 directions with 6 non-diffusion (b0) scans.

2.2 Paradigm: dichotic listening (DL) task

The DL paradigm has been used several times by Professor Mulert and colleges from the Psychiatry Neuroimaging Branch, Department of Psychiatry and Psychotherapy, University Medical Center Hamburg-Eppendorf, Hamburg, Germany. (e.g. Steinmann et al. 2014a)

The Bergen DL paradigm was used (Hugdahl and Andersson 1986, Hugdahl 2003), in which pairs of two consonant-vowel (CV) syllables (ba, da, ga, pa, ta, ka) were presented simultaneously at about 75 dB, one to each ear. The voiced syllables (ba, da, ga) had a short voice onset time (VOT) of 17 to 32 ms. The unvoiced syllables (pa, ta, ka) had a long VOT of 75 to 80 ms. VOT represents the time from the release of a consonant to the onset of the voicing. In order to reduce confounding effects that may arise from combining two CV with different VOT lengths, (Rimol et al. 2006) short VOT CV combinations with long VOT CV were excluded, leaving 12 possible pairs (six short/short and six long/long). Each pair was temporally modified to match the onsets of the initial consonants. The entire length of each syllable was 400 to 500 ms. All syllables were articulated with constant intonation and intensity by a German male speaker.

Two blocks of 120 trials each were presented to each participant during the experiment. The participants were instructed to select the syllable they heard on each trial, using a computer mouse with their right hand. The fact, that each ear received a different CV presented was not communicated with the participants. The number of correct RE and LE reports was registered. A laterality index (LI) for each participant was calculated using the formula LI=100*(correct RE reports – correct LE reports)/(correct RE reports + correct LE reports) (adapted from Hugdahl and Andersson 1986). The LI value ranges from -100 to +100, while 100 represents the highest REA and -100 the highest left ear advantage (LEA) (Rimol et al. 2006).

2.3 EEG recording and processing

The EEG reading was conducted in a sound-proof and electrically shielded environment, using a 64 channel ActiCap system (recording apparatus: Brain Products GmbH, Munich, Germany). EEGs were conducted using the same parameters and systems that were in use by the research group in previous studies such as Steinmann et al. (2014a). Electrodes-positioning in an extended 10/20 system of 64 electrodes (plus one reference and one ground electrode) was used. Four EOG channels were used to monitor eye movements (one lateral of the left eye, three for the right eye: lateral, above, below). Data were collected at a rate of 1000 samples per second. For EEG "SuperVisc electrode gel" (EASYCAP GmbH, Herrsching, Germany) have been used. All impedances were kept below 5 kΩ.

Subjects received auditory inputs through closed system headphones (Sehnheiser, HAD 200). Recordings were conducted using Brain Vision Recorder 1.10 (Brain Products, Munich, Germany).

As in previous studies of the group, the software "Brain Vision Analyzer 2.0" (Brain Products, Munich, Germany) have been used for offline processing. Data was Butterworth zero phase bandpass filtered from 20 to 120 Hz (IIR, 12dB/octave) and down sampled to 500 Hz. Channels were reoriented to common average. Epochs with artefacts due to muscle activity, sweat or movement in any channel were detected automatically by the software (amplitude threshold of 95 μV) and then checked manually and discarded (Picton et al. 2000). Subjects with more than three bad channels were excluded. In order to remove blinks and similar artefacts, Independent Component Analysis (Carl et al. 2012) was used. In order to adjust to artefacts due to miniature saccades in gamma band (Yuval-Greenberg et al. 2008) a “radial electro-oculogram channel” (REOG) was created according to the method described by Keren et al. Segments of EEG measurements have been then divided to RE and LE reports. Only correct reports (i.e. vowel was one of the two presented to one of the ears) were further analysed.

EEG-based *functional connectivity analysis*

EEG processing took place within the software LORETA KEY: low-resolution electromagnetic tomography (Pascual-Marqui et al. 1994, Pascual-Marqui 2007b). LORETA KEY have been chosen since it has previously been used by the working group (Mulert et al. 2011, Steinmann et al. 2014a, 2017), allowing for a comparison of the results with those collected in previous studies. In addition, LORETA KEY is, compared with other 3D EEG/MEG softwares, the one with the lowest localisation error (Pascual-marqui 1999, Pascual-marqui et al. 2002).

Since the interhemispheric connectivity between the auditory cortices was studied, the main cortical structures of interest are the PAC and SAC. Therefore, four predefined ROIs by the LORETA library were used for EEG analysis:BA41 and BA42 on both RH and LH. These voxels are in standard MNI305 space of 6239 voxels which is in the same Talairach space as MNI152 that is used as standard space in the DTI analysis carried out by the FMRIB Software Library (FSL) (Evans

et al. 1992, Collins 1994). The resolution LORETA uses, as indicated by its acronym, is quite low: the voxels of the ROIs are of 5 mm^3. Within the FSL software, similar predefined ROIs were searched. For more information about the choice of the ROIs for the DTI analysis see section "*creating ROI masks*".

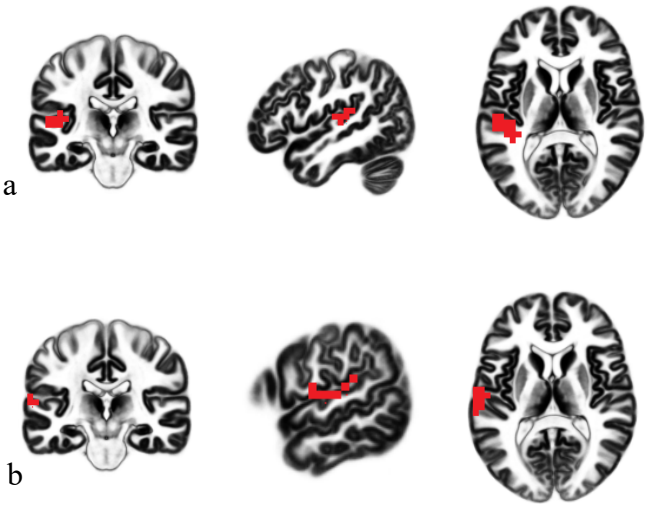

Fig. 4 a - b. **a**. ROI for BA41. **b**. ROI for BA42. ROIs are same for both hemispheres (mirrored). All ROIs are modeled here on an MNI152 brain using LORETA software.

LPS for each ROI pair (both HG; both pSTG) was calculated. Based on our previous DL work, in which we did not detect LPS differences in other frequency bands (delta, theta, alpha, beta) yet in the gamma range (30-100 Hz), analysis was focused on the entire gamma-band range in all correct left and right ear responded trials (i.e. bilateral).

The total LPS regarding a ROI is defined as the mean LPS for all voxel in the ROI for BA41 and all voxel in the ROI for BA42. The total LPS stands for the grade of connectivity of both ROIs. For all CV presentations, time frequency analysis was conducted applying a short-time-Fourier-transform (Bartlett-Hann window) using a 100 ms window width. This is in line with the LPS definition used by the group in past studies such as Steinmann et al. 2014a. LPS was obtained by that transformation using cross spectra. Results were extracted every 100 ms in a time frame from 0 to 800 ms after stimulus presentation and averaged to a single final mean value.

2.4 MRI Scans and processing

Structural imaging was performed using a T1-weighted 3D MPRAGE sequence covering the whole head. Protocol parameters were TE/TR = 2.98/2300 ms, TI 1100

ms, flip angle 9°, 256 × 192 × 240 matrix with FOV 256 × 192 × 240 mm^3 (acquisition time 7min 23s).

All scans were conducted in the same 3 Tesla MRI scanner (Magnetom TIM Trio model, Siemens, Erlangen, Germany) fitted with a gradient system producing a maximal field strength of 40 mT/m using a head coil of 12-channel within one cohort.
All probands were wearing MRI suitable headphones which were not connected to any source. The reason for using the headphones was to maintain standardisation with previous experimental design in which an fMRI sequence was also conducted. After canceling the fMRI sequence the usage of headphones and 12 channel coil have been kept to avoid confounding impacts. The main reason for canceling the fMRI was a significant discrepancy toward a left lateralisation between DL test in fMRI conditions and EEG conditions which was attributed to the loud sound made by the MRI scanner. This is consistent with the results of a study about the effects of noise on speech lateralisation using DL tasks (Dos Santos Sequeira et al. 2010). DTI data were obtained with echo planar imaging of the entire brain. The protocol parameter were as follows: TE/TR = 86/7700 ms, bandwidth = 1502Hz/Px, 104 × 128 matrix, FOV 208 × 256 mm^2, 64 axial slices, 2.0 mm slice thickness. Voxel size 2.0mm^2. Gradient pulses in 60 different directions were derived from a bucky ball with a b-value of 1000 s/mm^2. 6 Non-diffusion weighted images (b = 0 s/mm^2) were acquired after each tenth image to guide the processing of individual diffusion weighted images. (Le Bihan 2003, Koerte and Muehlmann 2014). To minimise the sensitivity considering frequency drifts, the measurement was devided into three acquisitions resulting in total scanning time of 9 min 39s.

DTI-based structural *connectivity analysis*

Data were processed using tools from FSL, (Jenkinson et al. 2012). DTI and MRI illustrations were created using MRI scans of the authors own brain of this thesis.

Converting *format of DTI*

Raw images in the DICOM (digital imaging and communications in medicine) format were fused together into the Neuroimaging Informatics Technology Initiative (NIfTI) format using the dcm2nii graphical user interface of the MRIcron software developed by Chris Rorden nitrc.org/projects/mricron/ 21.03.2017.

Merging *data*

In order to minimise sensitivity versus frequency drifts three acquisitions were performed, each of 20 b=1000 and two b=0 resulting after DICOM to NIfTI conversion in three separate directories for every subject. Each aquisition contained one NIfTI volume of 20 diffusion-weighted and two non-diffusion weighted images, one gradient table (bvecs) and one table of b values (bvals). In order to start the analysis, all three directories were merged to create one directory containing the three files. Merging the bvals was carried out by repeating the sequence three times using a simple text editing software so it would contain 66 entries instead of 22.

Each bvec file consists of three rows of entries and the entries are separated by blank spaces. Read horizontally, each row describes the parameters of the x, y and z-axis respectively. Every column describes one direction as a vector in three dimensions. Each tenth vector was a zero vector (0,0,0). In order to merge all three text files into one, the first row of the second file was copied and pasted at the end of the first row of the first file. The same was done with the second and third rows, and then all three copy paste actions for the third file. The final outcome was a text file containing three rows of 66 entries each. Merging all three NIfTI files was carried out by putting all three NifTI files in one directory and applying the FSLUTILS command:

*fslmerge -a dti.nii.gz *.nii.gz*

Creating a non-diffusion image

In order to create a non-diffusion weighted image, the following FSLUTILS command was used:

fslroi dti nodif 0 1

This separates the first 3D image, out of the volume of altogether 66 3D images, which is a non-diffusion image (T2 weighted).

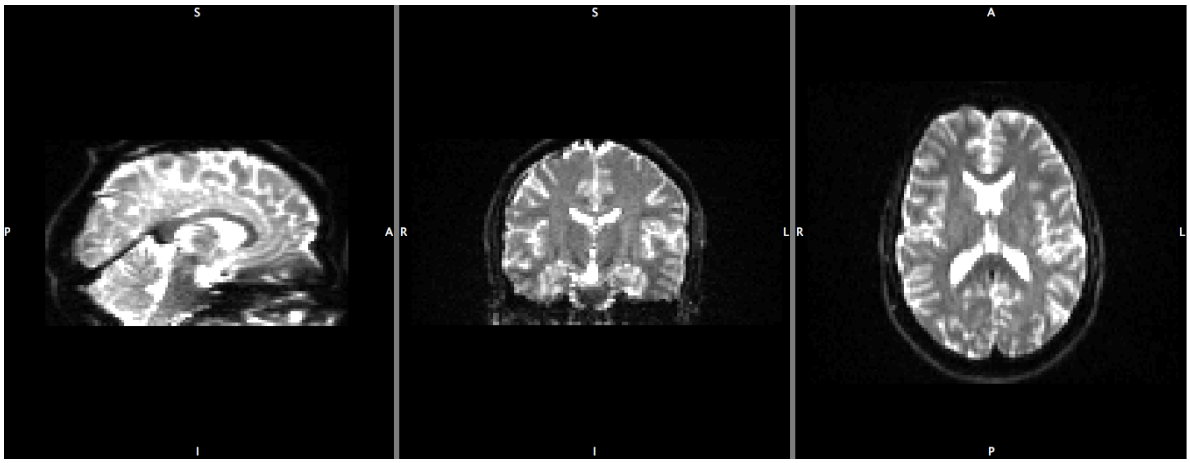

Fig. 5. Non-diffusion weighted image.

Brain extraction

Brain extraction was performed using the Brain Extraction Tool (BET) (Smith 2002, Jenkinson et al. 2005) of the FSL software set to a fractional intensity threshold of 0.2 using the following command:

bet nodif nodif_brain -m -f 0.2 -v

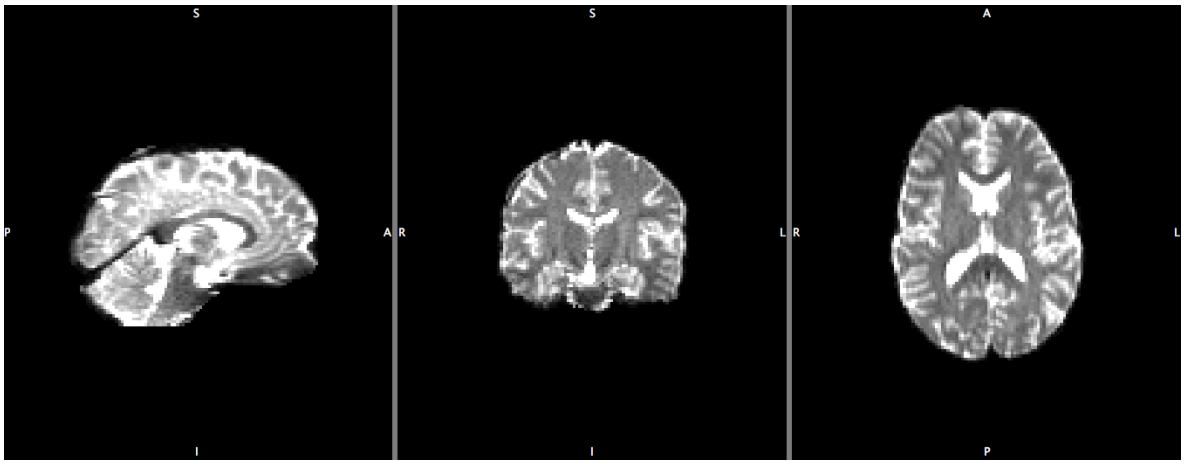

Fig. 6. Non-diffusion weighted image after removal of skull.

Eddy current correction

The gradient coils create shears and stretches, also known as eddy currents, which creates artefacts in diffusion weighted images. These artefacts are different for different images. Head motions are responsible for more artefacts. To correct for both eddy currents and head motions the FMRIB Diffusion Toolbox (FDT) (Behrens et al. 2003a, 2003a, 2007, Jbabdi et al. 2012) was used, which is a part of FSL using the following command:

eddy_correct dti data 0

This results in an affine (linear) registration with 12 degrees of freedom (DOF) as the first non-diffusion volume functions as a reference image. This is the same image that was separated to create a non-diffusion weighted image.

Gradient table rotation

Since every diffusion image was registered to the first non-diffusion image, the original bvecs file was no longer accurate. A script called fdt_rotate_bvecs.sh (created by Saad Jbabdi, https://www.jiscmail.ac.uk/cgi-bin/webadmin?A2=fsl;3777d8fe.1202 8.12.2016) was used to rotate the gradient table according to the latter registration using the following command:

fdt_rotate_bvecs bvecs rotbvecs data.ecclog

Tensor fitting

Maps of FA, mean diffusivity, eigenvectors (V1, V2, V3) and eigenvalues (L1, L2, L3) were calculated using the DTI fit utility of FDT using the following command:

dtifit -k data -o <id> -m nodif_brain_mask -r rotbvecs -b bvals

The output (*-o <id>*) was set to the pseudonymised name of the subject (e.g. -o V12108).

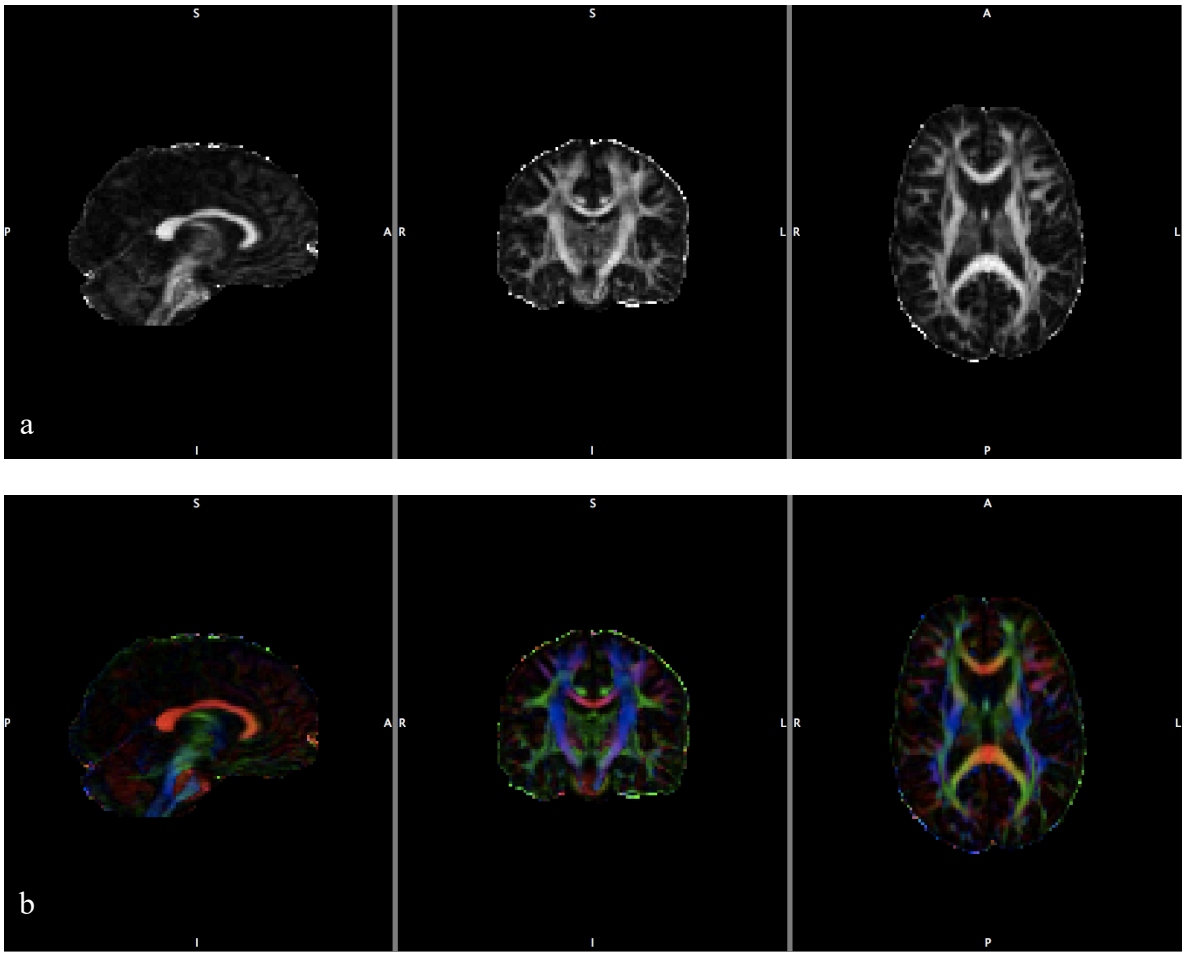

Fig. 7 a - b. **a**. FA image. **b**. FA image with colour coded directions: red: left-right, green: anterior-posterior, blue: superior-inferior.

Axial and radial diffusivity

The largest eigenvalue of each voxel is listed in the L1 map and is oriented parallel to the axon. This map is by definition equal to the tensor parameter axial diffusivity (AD) and requires no further modifications.

Since FDT Diffusion creates two separate maps for the second and third eigenvalues, both had to be averaged to create a map of radial diffusivity (RD). This was carried out using the following commands:

*fslmaths *L2 -add *L3 RD*
fslmaths RD -div 2 RD

The first command adds the first matrix (L2) to the second (L3) whereas the second command divides the resulting map by 2 to create an average map of L2 and L3.

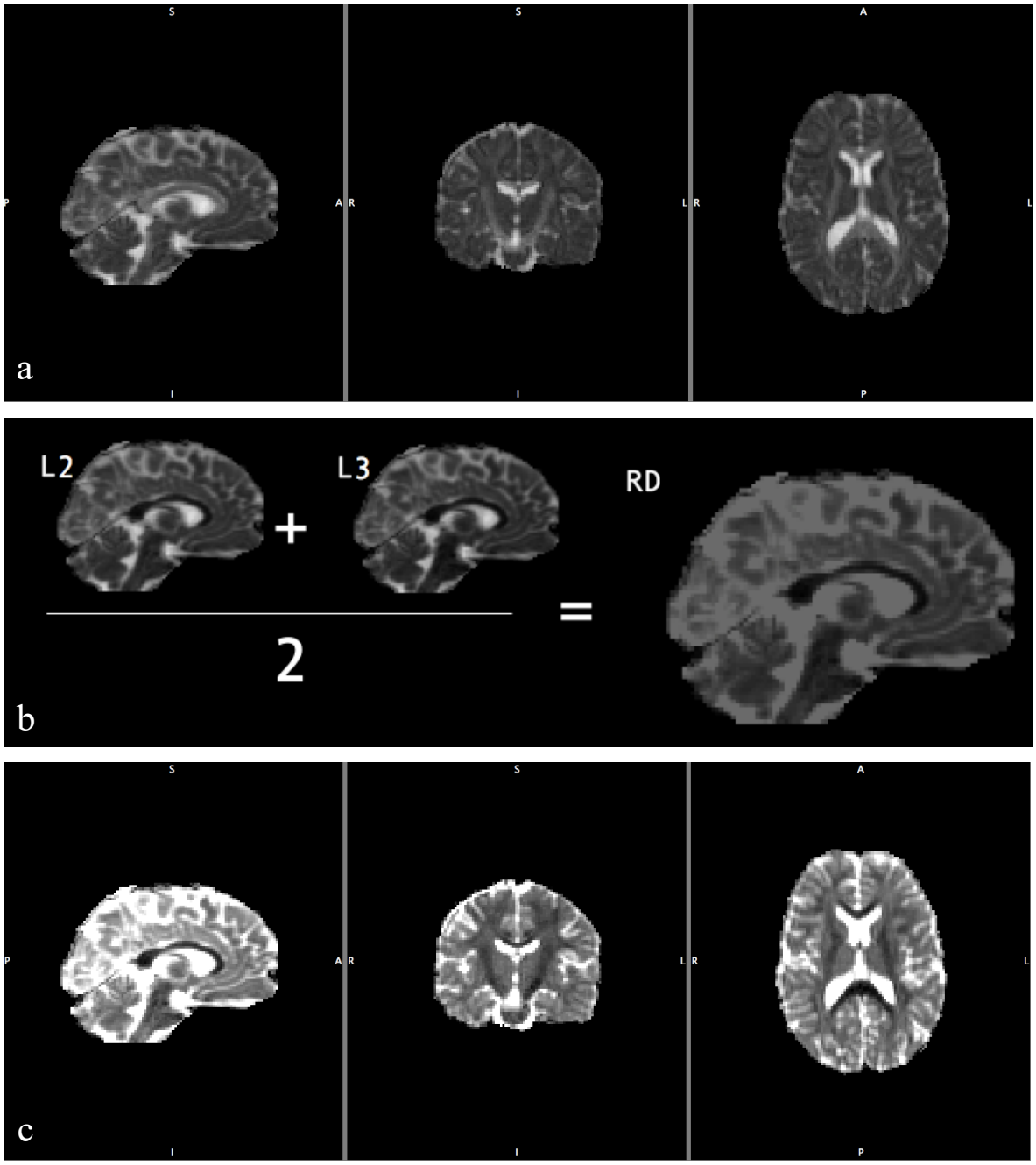

Fig. 8 a - c. **a**. AD image. **b**. Illustration of the creation of RD map by combining L2 and L3 into one image and dividing the intensity by 2. **c**. RD image.

Fibres orientation estimation

To quantify uncertainty, estimate fibres orientation and model crossing fibres the BEDPOSTX function of FDT (Behrens et al. 2003b, 2007) was applied. BEDPOSTX stands for Bayesian Estimation of Diffusion Parameters Obtained using Sampling Techniques. BEDPOSTX creates all files needed as a starting point for probabilistic tractography which would be carried later. To apply BEDPOSTX a directory named bedpostx was created. bvals, bvecs (renamed from rotbvecs), 4D volume (output of

eddy current correction) and a non-diffusion brain mask (output of BET) were put into the bedpostx directory and the following command was applied:

bedpostx bedpostx

Converting format of MRI and reorientation

The MRI raw data is in form of many DICOM files. These DICOM files were converted into a NIfTI volume using the dcm2nii software. The same software was used to reorient the image to the nearest orthogonal to achieve the same orientation as in the DTI data.

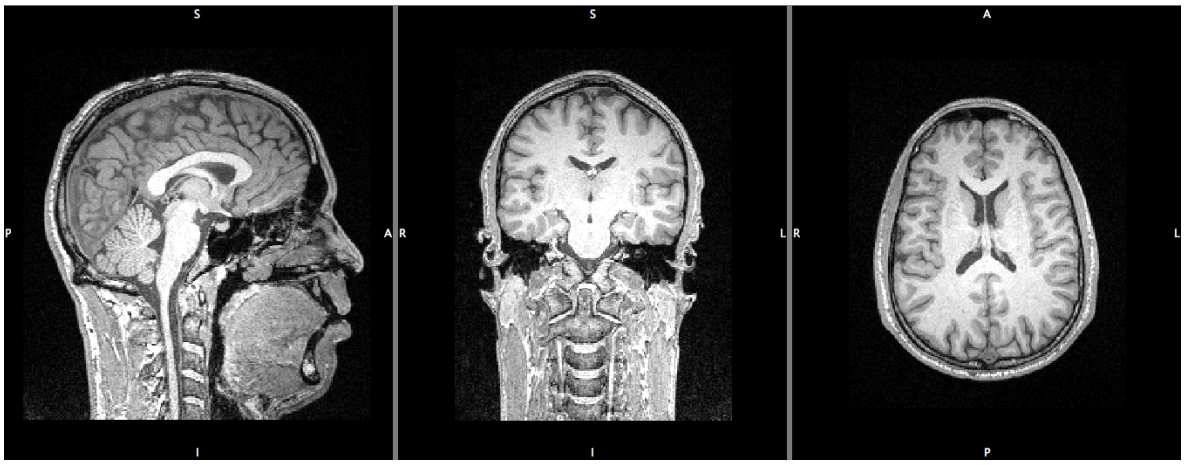

Fig. 9. T1 weighted MRI image.

Brain extraction of MRI

In order to perform a brain extraction using BET (Smith 2002), a fractional intensity threshold of 0.6 was set. First, a starting point had to be defined as the brain centre. After a series of calibration trials, It have been decided to set the brain centre to be the superior posterior voxel of the CC of the midsagittal slice. This was applied using the following command:

bet MRI MRI_brain -m -f 0.6 -v -c <x y z>

Where *<x y z>* was replaced by the coordinates of brain centre as described above.

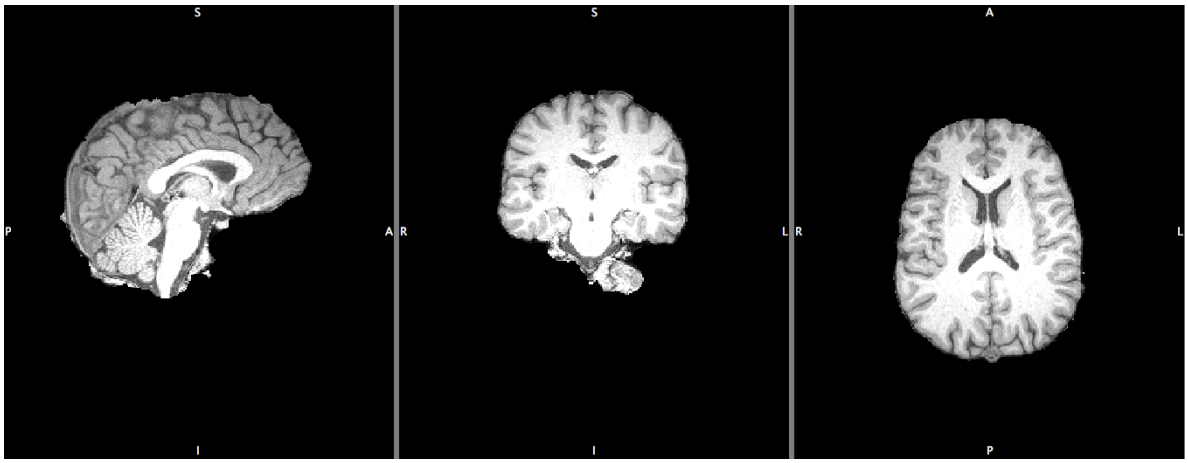

Fig. 10. T1 weighted MRI image after removal of the skull.

Registration

The registration was performed between structural (MRI), diffusion (DTI) and standard space (MNI 152) with resolutions of 1, 2, and 1 mm^3 respectively. The transformation between diffusion and structural spaces were carried out using 6 DOFs (3 rotations and 3 translations, AKA rigid body registration), between structural and standard space using 12 DOFs (3 rotations, 3 translations, 3 shearings and 3 scalings, AKA affine). A non-linear registration was carried out between structural and standard as well as between diffusion and standard spaces. The idea of registration is to align different brains (i.e. MNI 152 standard brain and one of a subject) or different images of the same brain to each other. Within two images registered to same space, same coordinates should represent the same structure in both brains (i.e. in a diffusion image transformed into MNI 152 space, the coordinates of the CC in the former image should match those of the latter).

flirt -in nodif_brain -ref MRI_brain -omat diff2str.mat -searchrx -90 90 -searchry -90 90 -searchrz -90 90 -dof 6 -cost corratio

convert_xfm -omat str2diff.mat -inverse diff2str.mat

flirt -in MRI_brain -ref MNI152_T1_1mm_brain -omat str2standard.mat -searchrx -90 90 -searchry -90 90 -searchrz -90 90 -dof 12 -cost corratio

convert_xfm -omat standard2str.mat -inverse str2standard.mat

convert_xfm -omat diff2standard.mat -concat str2standard.mat diff2str.mat

convert_xfm -omat standard2diff.mat -inverse diff2standard.mat

fnirt --in=MRI --aff=str2standard.mat --cout=str2standard_warp --config=T1_2_MNI152_2mm

inwarp -w str2standard_warp -o standard2str_warp -r MRI_brain

convertwarp -o diff2standard_warp -r MNI152_T1_2mm -m diff2str.mat -w str2standard_warp

convertwarp -o standard2diff_warp -r nodif_brain_mask -w standard2str_warp --postmat=str2diff.mat

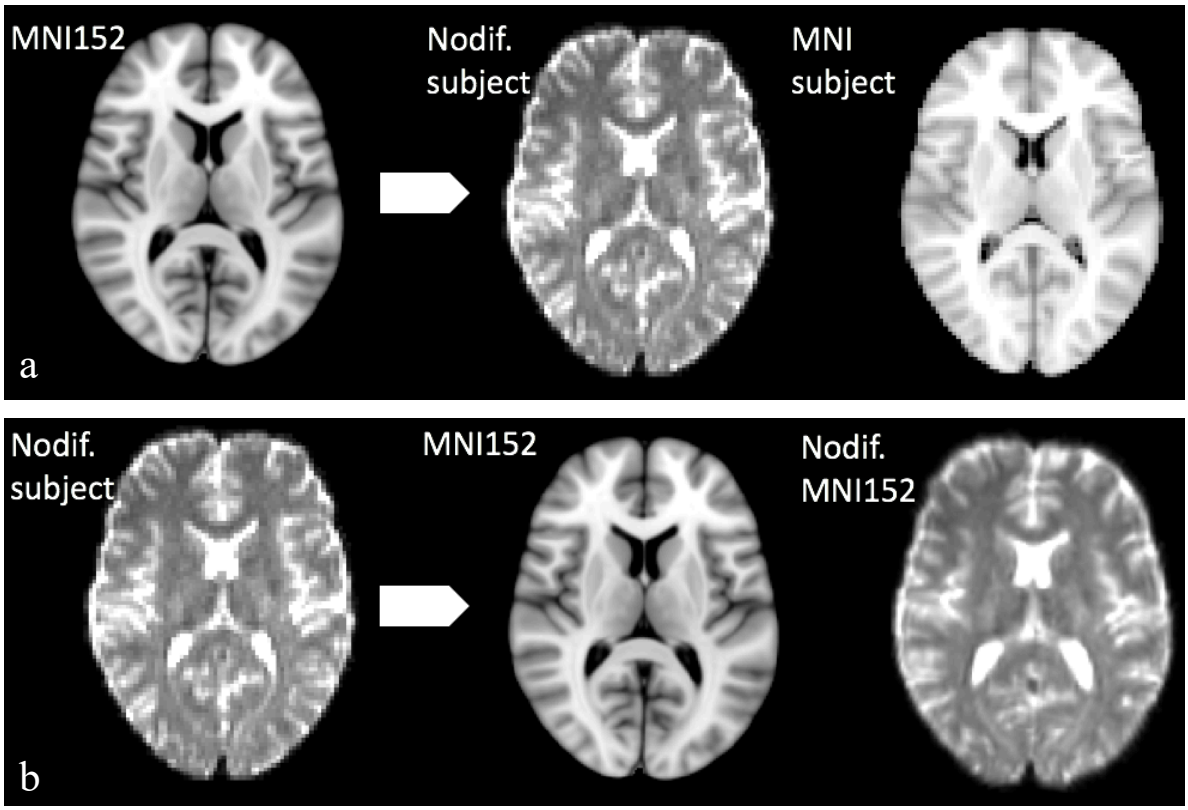

Fig. 11 a - b. **a**. Registration of an MNI152 brain in individual diffusion space. **b**. Reverse registration of non-diffusion image in standard space.

Creating ROI masks

The goal of this study was to track fibres between HG and pSTG that cross through the CC. Therefore following masks had to be produced: 1) HG of the RH, 2) HG of the LH, 3) pSTG of the RH 4) pSTG of the LH and 5) a midsaggital mask of the CC.

The masks were first obtained using the Atlas tool of FSLVIEW of the FSL software. First, an MNI152 1mm standard was opened using FSLVIEW and created probability maps of HG (which is roughly identical with BA41) and of pSTG using the "Harvard-Oxford cortical structural atlas" (Desikan et al. 2006). Both structures were extracted and saved as images. Since such usage of an atlas is a probabilistic assumption, a probability threshold had to be defined. This was set to a minimum of

20%. The images of both structures were then processed so that every voxel under 20 would become zero, and then binarised. This was carried out using the following commands:

fslmaths pSTG -thr 20 -bin pSTG
fslmaths HG -thr 20 -bin HG

The next step was removing every voxel on pSTG that is covered by HG in order to receive a Mask of the pSTG which is roughly identical with BA42. This was done using the following command:

fslmaths pSTG -sub HG -bin pSTG

In order to isolate masks for RH and LH respectively, following commands were applied:

fslmaths HG -roi 90 -1 -1 -1 -1 -1 -1 -1 HG_L
fslmaths HG -roi -1 90 -1 -1 -1 -1 -1 -1 HG_R
fslmaths pSTG -roi 90 -1 -1 -1 -1 -1 -1 -1 pSTG_L
fslmaths pSTG -roi -1 90 -1 -1 -1 -1 -1 -1 pSTG_R

The value 90 results of the fact that there are 181 voxels in the x direction. 90 is about halfway.

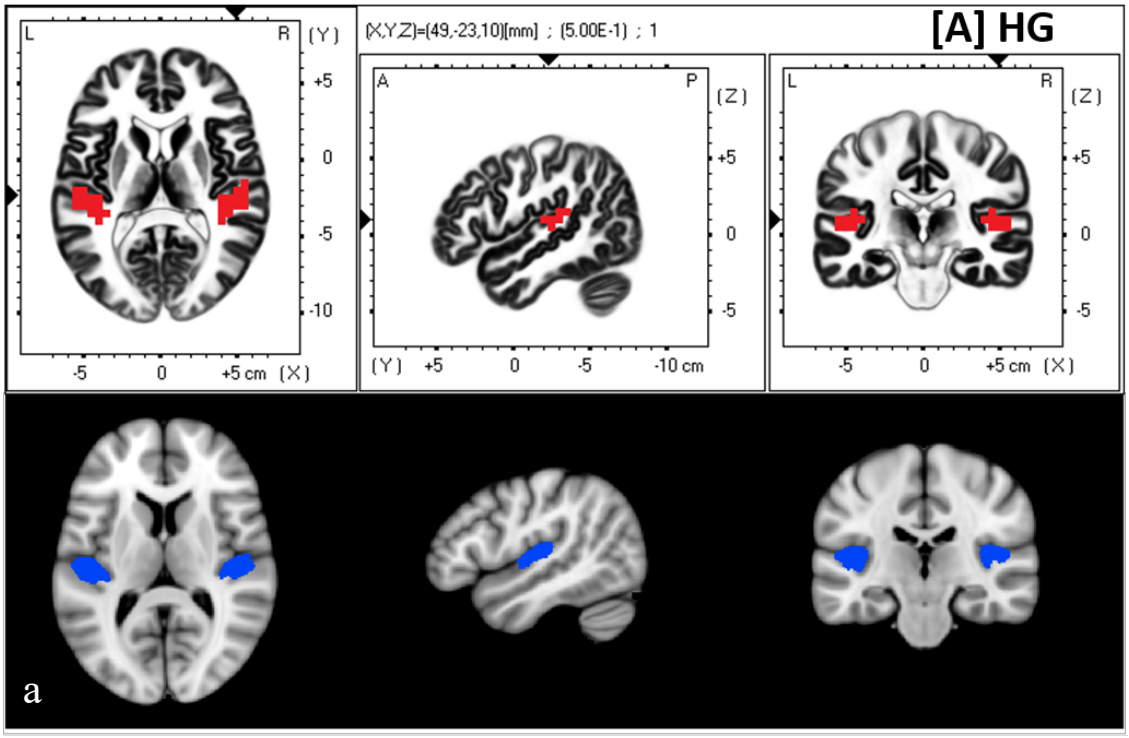
[A] HG
(X,Y,Z)=(49,-23,10)[mm] ; (5.00E-1) ; 1
L
R
(Y)
(Z)
A
P
+5
0
-5
-10
-5 0 +5 cm (X)
(Y) +5 0 -5 -10 cm
a

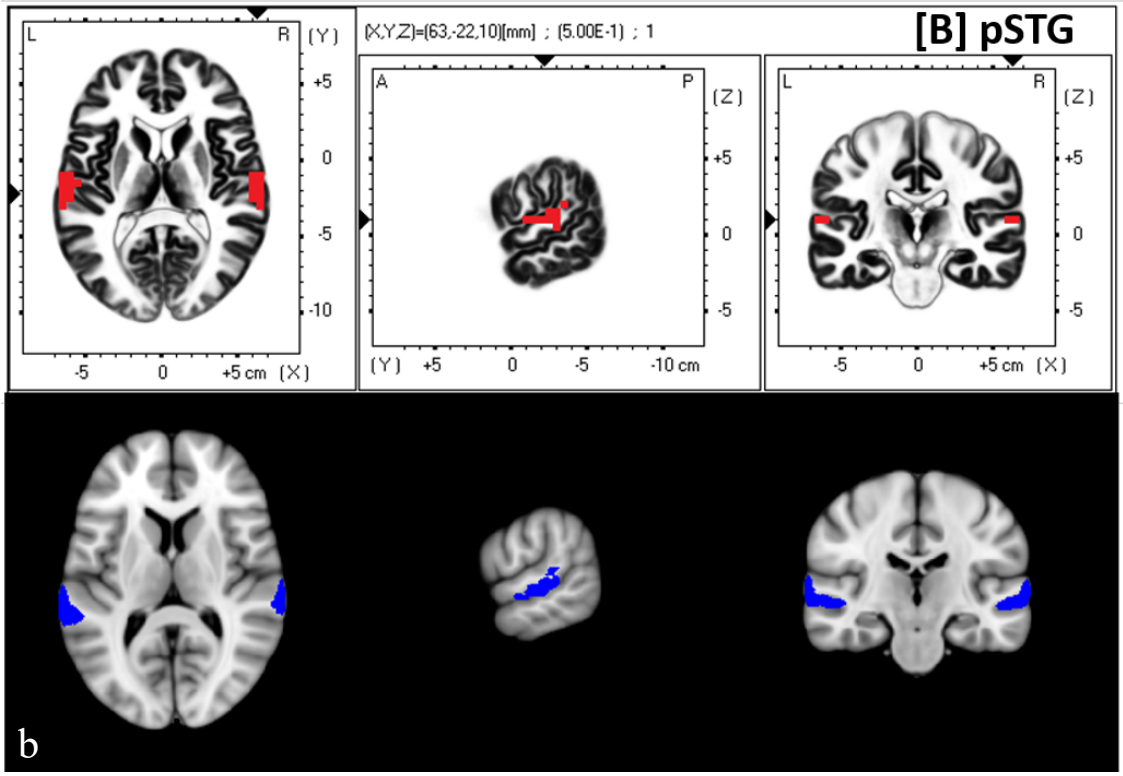
[B] pSTG
(X,Y,Z)=(63,-22,10)[mm] ; (5.00E-1) ; 1
L
R
(Y)
(Z)
A
P
+5
0
-5
-10
-5 0 +5 cm (X)
(Y) +5 0 -5 -10 cm
b

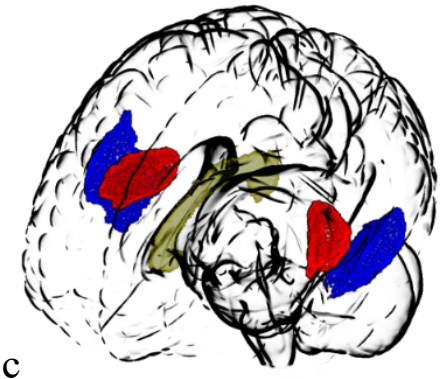

c

Fig. 12 a - c. White background: ROIs created using the LORETA software. Black background: ROIs created in FSL in standard space. **a**. BA41 / HG. **b**. BA42 / pSTG. **c**. 3D illustration of pSTG (blue) HG (red), and a midsagittal cut of the callosal body (yellow).

Transforming masks into structural space

To allow further adjustments, all four masks were first transformed into the structural space of each subject and then binarised. The following commands were used: (example for HG_L)

applywarp -i HG_L -r MRI_brain -o HG_L -w standard2str_warp
fslmaths HG_L -bin HG_L

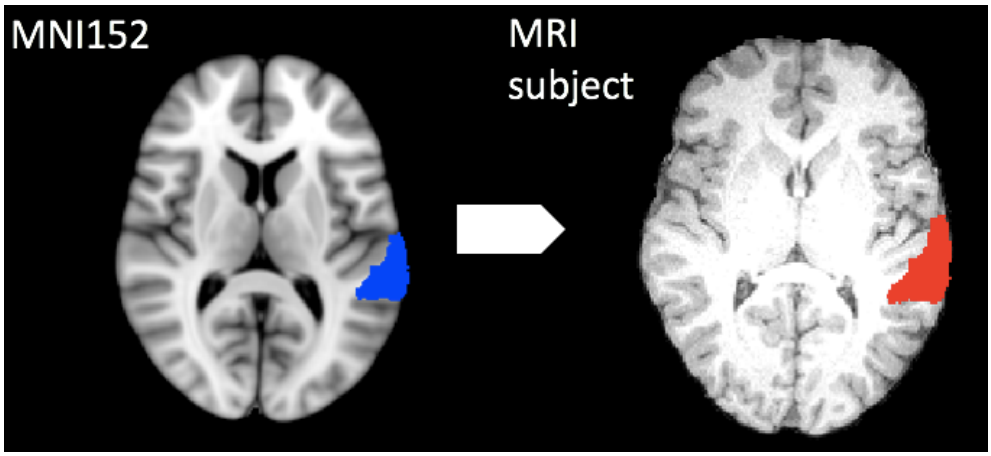

Fig. 13. Registration of the ROI of the left HG from standard space into individual structural space of MRI image.

MRI segmentation

Segmentation of MRI images into CSF, WM and cortex was carried out using the FAST tool of FSL. Then, the image of the cortex was binarised, so the image would contain only voxels with the value 0 or 1. The following command was used:

fast -t 1 -n 3 -H 0.1 -I 4 -l 20.0 -o MRI MRI

fslmaths cortex -bin cortex

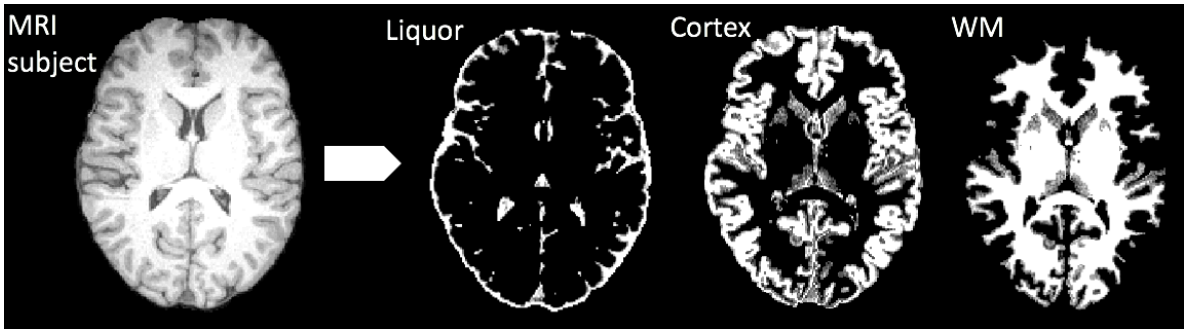

Fig. 14. Segmentation of an individual T1 weighted MRI volume of a subject into CSF, cortex and WM.

Masks limitation to cortex

In order to restrict masks to cortical areas only, the cortical image was first binarised and then multiplied with each mask using the following command: (example for HG_L_str)

fslmaths cortex -mul HG_L –bin HG_L

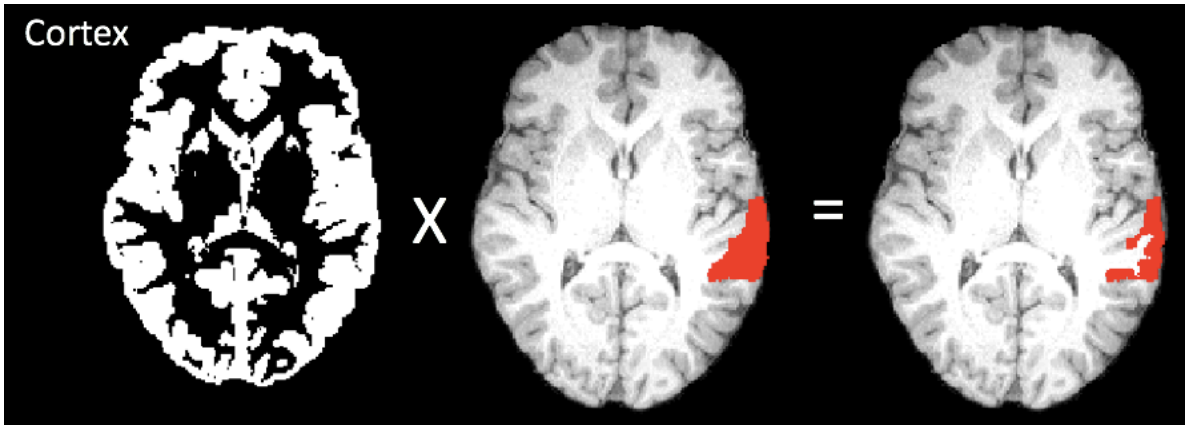

Fig. 15. Multiplication of a binarised Cortex mask with the initial left HG ROI. New ROI is restricted to cortex area.

Transforming masks into diffusion space

In order to conduct probabilistic tractography, masks had to be first transferred into diffusion space and then binarised. This was done using the following commands:

flirt -in HG_L_cortex -applyxfm -init str2diff.mat -out HG_L -paddingsize 0.0 -interp trilinear -ref nodif_brain

fslmath HG_L -bin HG_L

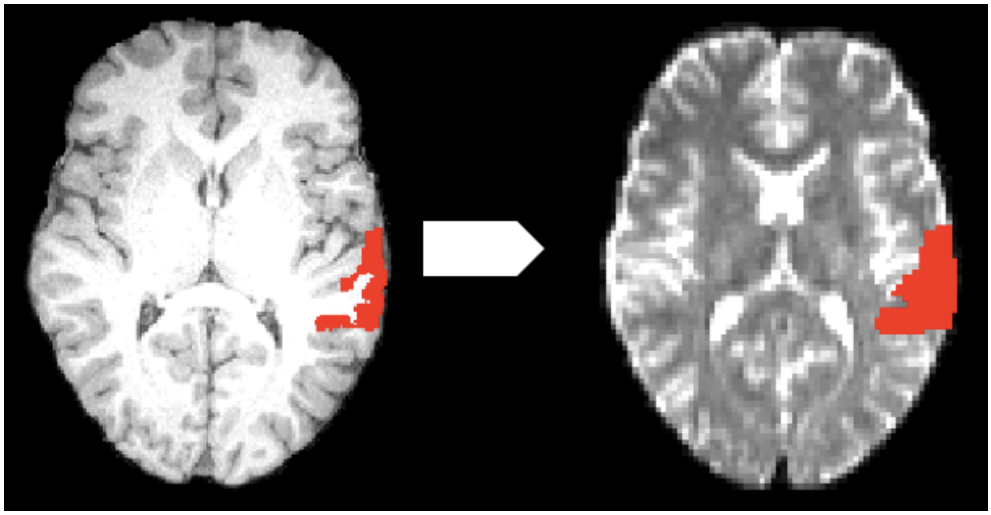

Fig. 16. Registration of ROI of the left HG into diffusion space. The resulting ROI is the final one and will be used for the probabilistic tractography.

Creating a callosal mask

In order to create a callosal mask an image of the CC named "WM Callosal body" was created from the "Juelich Histological Atlas" of the FSL View software, and then thresholded for 20-100% and binarised. The adjustment took part in standard space on a 1mm^3 MNI152 Brain.

fslmaths CC -thr 20 -bin CC

The image were then transformed into the diffusion space of each proband and then a midsagittal cut of the 3D image into one 2D image (X=64 out of 127) was done to create a 2D mask by multiplying the 3D image with a mask in which every voxel (64;y;z), i.e. every voxel for which the coordinate x equals 64, has the value 1 while all other voxels has the value 0.

The command for registration of the mask was:

applywarp -i CC –r nodif_brain –o CC –w standard2diff_warp

fslmaths CC -mul X64 –bin CC

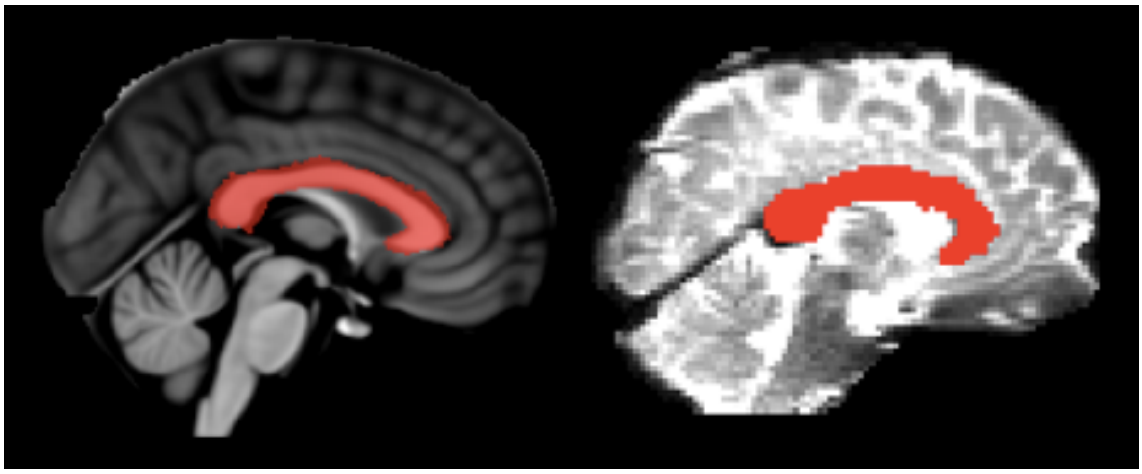

Fig. 17. Left: Image of the CC, created with the atlas tool of fslview on the midsagittal view (x=91 out of 181). Right: CC registered into individual diffusion space, presented on a non-diffusion image.

Probabilistic tractography

In order to examine the connection between both hemispheres, probabilistic tractography had to first be implemented. The following tracts have been processed via PROBTRACKX of FDT: 1) HG_R -> HG_L, 2) HG_L -> HG_R, 3) pSTG_R -> pSTG_L 4) pSTG_L -> pSTG_R. The tracts have been named Track1 Track2 etc. respectively. A curvature threshold of 0.2 was chosen and the step length was set to 0.5 mm. Waypoint condition was set to "AND", i.e. only fibres going through both masks and through the CC appear in the tractography. The tracts were set to terminate at the target mask. In order to save time by tracking only within the brain area, an exclusion mask FAO was defined containing all voxels outside of the brain (every voxel outside of the brain gets the value 1 and every voxel inside the value 0).

Creating the exclusion mask FAO:

fslmaths nodif_brain_mask -mul -1 -add 1 FAO

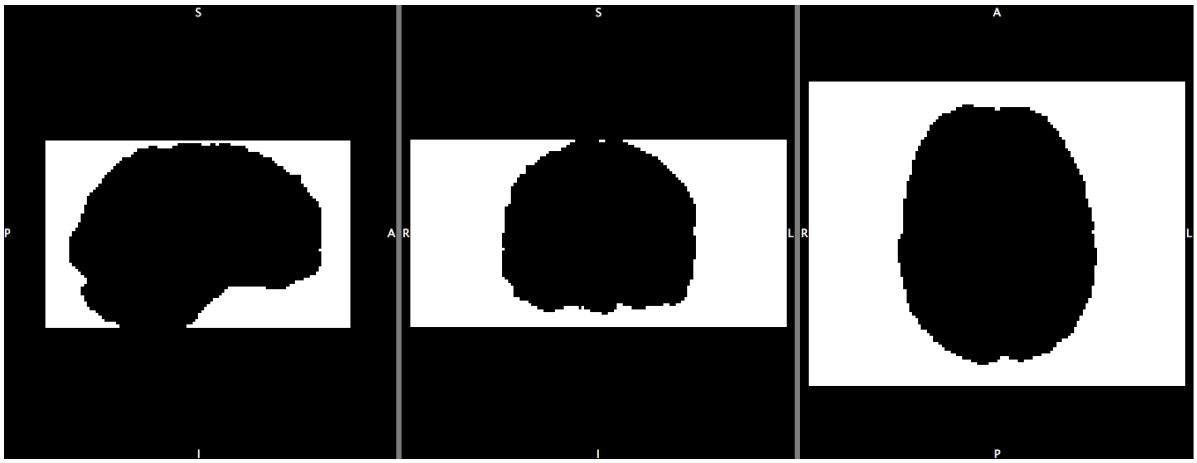

Fig. 18. FAO mask.

Following commands were applied to conduct each tractography (e.g. Track1):

mkdir Track1

printf '%s\n' 'HG_L' 'CC' >Track1/waypoints1.txt

/usr/local/fsl/bin/probtrackx2 -x HG_R -l --onewaycondition -c 0.2 -S 2000 --steplength=0.5 -P 5000 --fibthresh=0.01 --distthresh=0.0 --sampvox=0.0 --avoid= FAO --stop=HG_L --forcedir --opd -s bedpost.bedpostX/merged -m bedpost.bedpostX/nodif_brain_mask --dir=Track1 --waypoints=Track1/waypoints1.txt --waycond=AND -V 1

2.5 Extracting tractography final results

The idea of the tractography was to see where the fibres are crossing. The following presents the procedure of getting statistical information of the neuronal connection.

Fibre tracts processing

In order to process with the mathematical analysis, tracts needed first to be normalised. To do so, the intensity of each voxel was divided by the number of fibres calculated for the tract. This number is specified in the file "waytotal" that was created in probtrackx. The following command was applied to every tract:

fslmaths –fdt_paths -div `cat waytotal` fdt_paths_norm

Furthermore, a probability threshold of 1% was chosen and the tracts were thresholded. The following command was applied to every tractography:

fslmaths –thr 0.01 fdt_paths_norm fdt_paths_0.01

Tracts connecting two corresponding ROIs (i.e. HG_L with HG_R, etc.) were combined into one tract and binarised.

fslmaths Track1/fdt_paths_0.01 –add Track2/fdt_paths_0.01 paths_HG
fslmaths paths_HG –bin paths_HG

Creating a volume of FA within the tracts

The binarised tracts path_HG and path_pSTG were multiplied with the FA map of each subject to create a FA map restricted to where the fibres connecting both structures pass.

fslmaths paths_HG -mul FA paths_HG_FA

Calculating FA values

Calculating mean non-zero FA within the HG and pSTG connecting tracts.

fslstats paths_HG_FA -M
fslstats paths_pSTG_FA -M

2.6 Statistics

SPSS 24.0 was used for statistical analysis. An analysis of covariance (ANCOVA) was carried out for age regarding FA of male and female to control for interfering effects, since these are known to influence FA values (Salat et al. 2005, Sullivan and Pfefferbaum 2006, Inano et al. 2011). One tailed Bonferroni-holm corrected correlations were conducted in order to interpret axon architecture, respectively gamma synchrony relations with hearing lateralisation (i.e. FA, LPS and DL

performance (LI, LE / RE reports). 95% confidence interals (CI) were calculated by Bootstrapping regarding each significant correlation.

3. Results

3.1 Demografic and behavioural DL performance

Of the thirty participants, three were excluded from analyses because of hearing problems or due to technical artefacts, such that 27 participants were included in final analyses. Overall, in 55.9% of CV presentations resulted in RE reports and 33.8% in LE reports. This implies an expected right ear advantage (mean Laterality-Index 23.56 ; SD 19.70). Within 10.3% of all CV presentations, the CV was wrongly reported by the subject, as it was not presented at all to any ear. Within 23 of the 27 subjects presented a positive laterality index. Four subjects presented a negative laterality index. Further, time between CV presentation and reporting was shorter for RE (mean 2.89 s) in comparison with LE (mean 2.99 s).

3.2 DL and DTI: Laterality Index, Correct reports and Fractional Anisotropy

Relating the dichotic listening performance to the results of the probabilistic tractography, a negative correlation was detected between the FA of the pSTG tract and LI ($r = -.412$, Bonferroni-holm corrected $p = .032$, bootstrap CI = -.657 to -.088). Analysing the number of LE and RE correct reports separately, we found a significant correlation between pSTG-based tracked FA and LE reports ($r = .345$, Bonferroni-holm corrected $p = .039$, bootstrap CI = .041 to .628, while a negative correlation was found with RE reports ($r = -.454$, Bonferroni-holm corrected $p = .027$, bootstrap CI = -.687 to -.157, see Figure 4A). Such association could not be found between HG-based tracked FA values ($p > 0.10$).

3.3 DL and EEG: Laterality Index, correct reports and Lagged Phase Synchronisation

Interhemispheric LPS between homologue pSTG was correlating negatively with LI ($r = -0.559$, Bonferroni-holm corrected $p = 0.006$, bootstrap CI = -0.791 to -0.189) and this relationship was also observed with the number of correct RE reports ($r = -0.625$, Bonferroni-holm corrected $p = 0.005$; bootstrap CI = -0.827 to -0.285), while a significant positive correlation was found with the number of correct LE reports (r

= 0.454, Bonferroni-holm corrected p = 0.018; bootstrap CI = 0.052 to 0.749). LPS between homolog HG correlated negatively with LI (rho = -0.488, Bonferroni-holm corrected p = 0.015, bootstrap CI = -0.754 to -0.109) and also with the number of RE reports (rho = -0.571, Bonferroni-holm corrected p = 0.004, bootstrap CI = -0.794 to -0.233), while the number of LE reports were positively correlated (rho = -0.413, Bonferroni-holm corrected p = 0.016, bootstrap CI = 0.019 to 0.728) (see Figure 19.B).

3.4 DTI and EEG: Fractional anisotrophy and Lagged Phase Synchronisation

Other than expected, analysis could not detect a significant correlation between gamma-band-synchrony and mean FA within the interconnecting pathway connecting HG and pSTG. See figure 19.C. A regression-analysis for the pSTG connecting pathway, examining laterality index against FA, MD, AD, RD and LPS concluded that only LPS (beta: -0.496 for t(24): -3.08; p: 0.005) and FA (beta: -0.311 for t(24): -1.93; p: 0.065) were contributing predictors for LI (F(24): 8.177; p: 0.002). Furthermore, LPS have been better than FA at predicting LI (beta of LPS: -0.496; beta of FA: -0.311), almost reaching significance (p: 0.65).

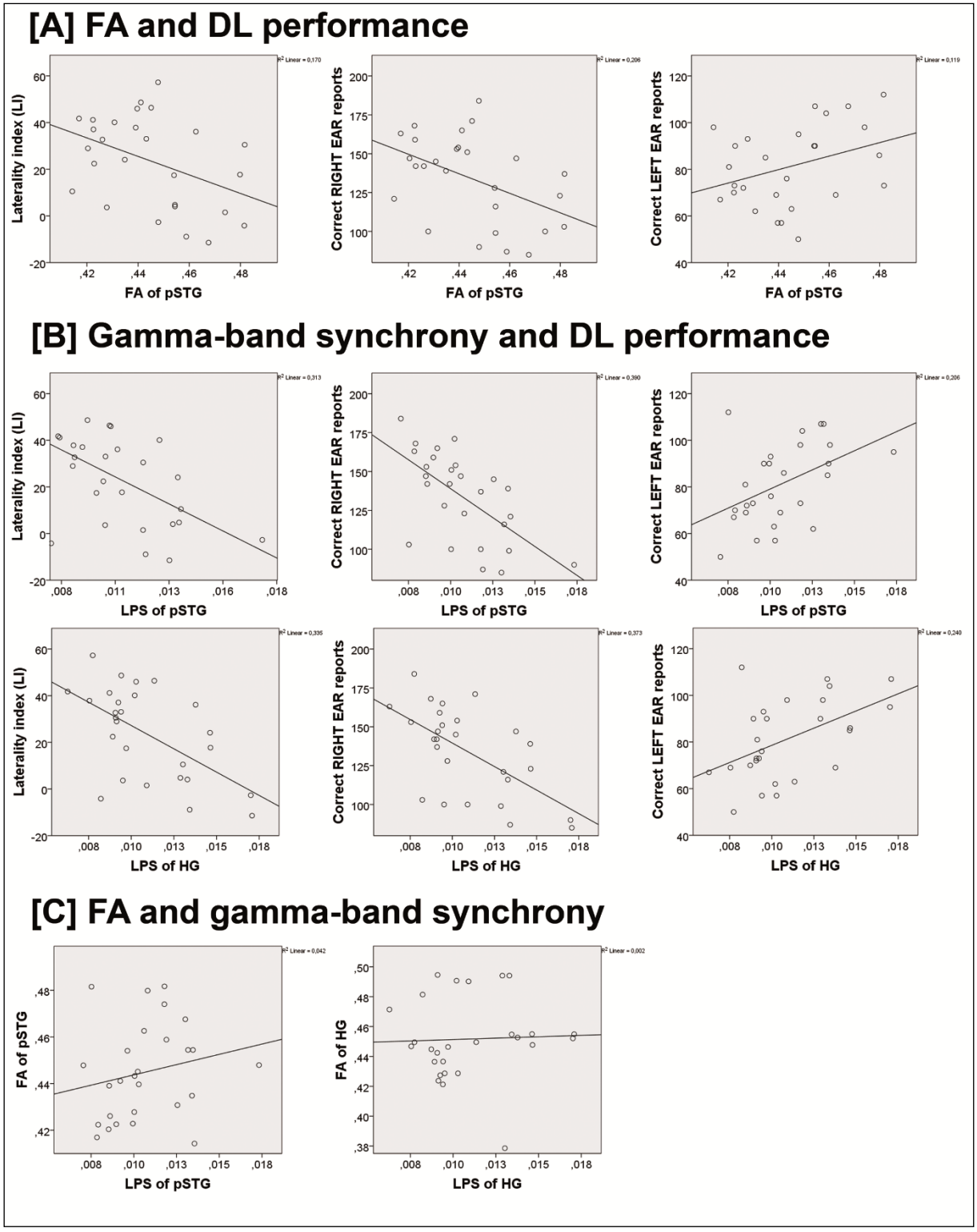

Figure 19 A - C. Scatterplots displaying the significant association between **[A]** the mean fractional anisotropy (FA) value of the interhemispheric auditory pathway connecting homolog pSTG, or **[B]** the mean gamma-band synchrony (lagged phase synchronization/ LPS) connecting either pSTG or HG, and the dichotic listening performance (all $p < 0.05$). **[C]** Scatterplots dispaying the non-significant association between LPS and average FA values regarding the interhemispheric auditory pathway linking both pSTG or both HG.

3.5 Connecting Tracts

DTI fiber tracking

Fiber tracking results are presented on a MNI152 standardised brain in Fig. 20, confirming that the interhemispheric auditory pathways connecting the HG or pSTG of one hemisphere and the other pass through the callosal bodies. The analysis of covariance with correction for age have not exposed any significant FA discrepancy for a certain sex ($p > 0.12$).

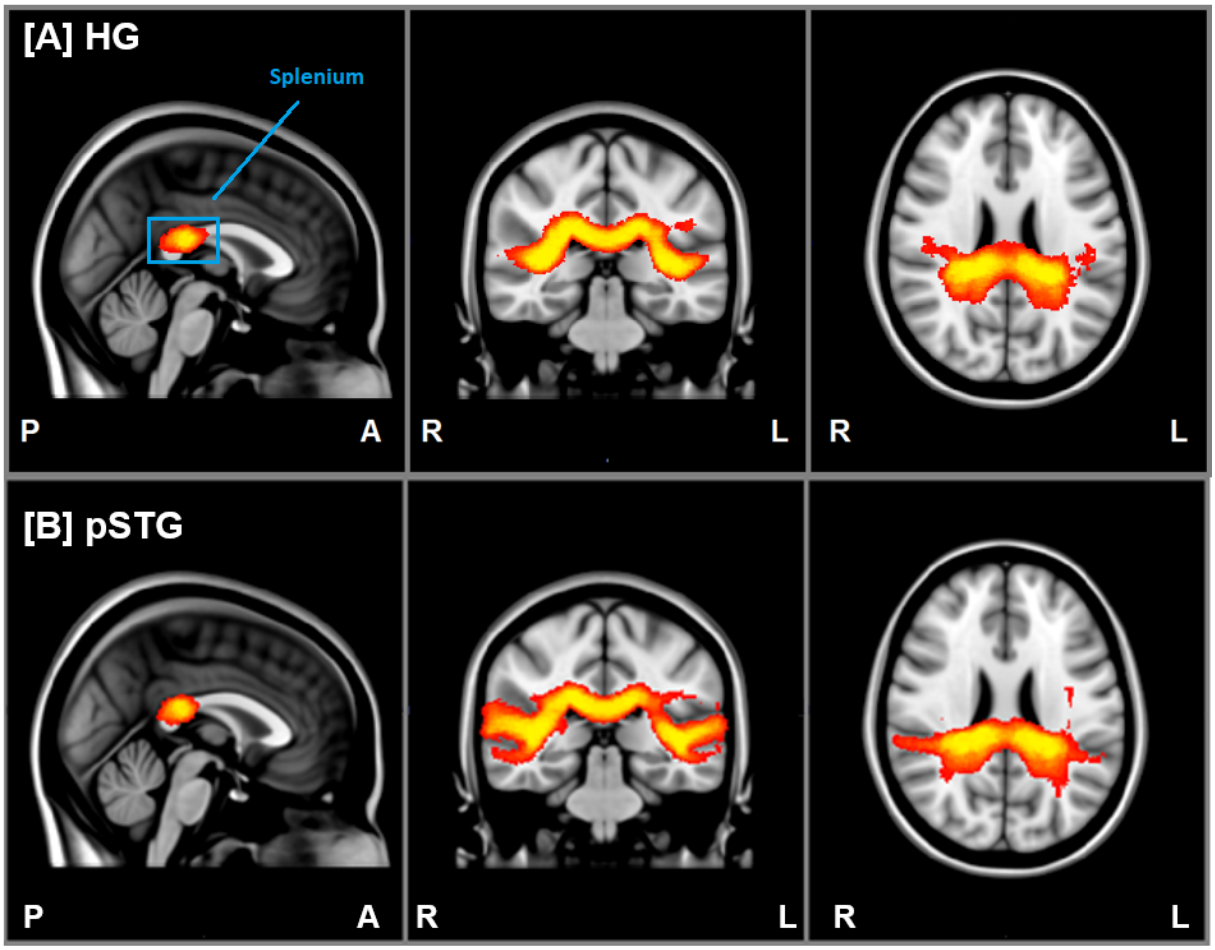

Figure 20 A - B. Group mean tractographies displayed on a single standardised Brain. Cumulated fiber densities of each voxel linking **[A]** Heschl's gyrus (HG) and **[B]** posterior superior temporal gyrus (pSTG) on both hemispheres in standard space (MNI152). The intensity (red-yellow scale) correspond to the number of tracks passing through each of the voxels. A: anterior; P: posterior; R: right; L: left.

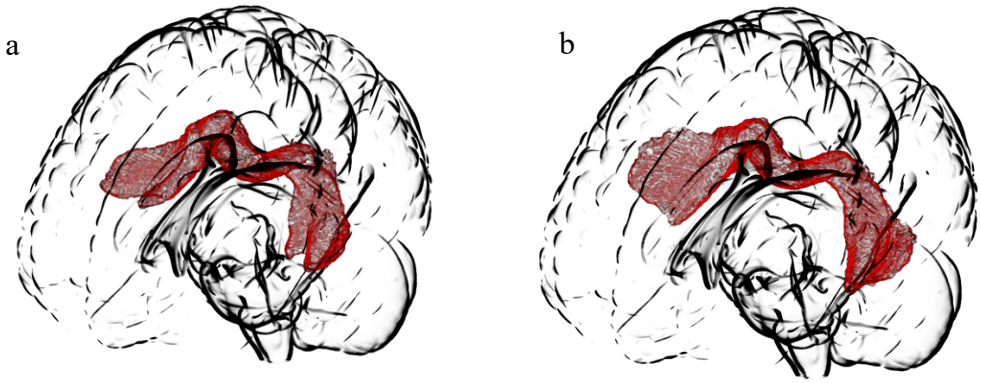

Fig. 21 a - b. **a**. All tracts connecting HG superpositioned in 3D. **b**. All tracts connecting pSTG superpositioned in 3D.

4. Discussion

Although the interhemispheric connectivity between bilateral auditory cortices has been a matter of neurophysiological research, no multimodal study so far exists investigating both structural and functional connectivity within a single group of participants as presented in this doctoral thesis. In this research, we combined DTI based fiber tracking of the interhemispheric auditory connection, EEG based gamma-band coherence, and dichotic listening performance of 27 healthy volunteers to examine the role of this pathway in relating the synchrony of gamma-band which is crucial for acustic perception of syllables perceived by the left ear. The main findings of this project are correlations between functional, structural and behavioural variables, regarding DL that support two of our main hypothesis: (1) higher FA within the interhemispheric auditory pathway and (2) higher gamma-band synchronization between pSTG on both hemispheres were both linked to diminished language lateralisation. Nevertheless, there was no significant association between the endpoints of both imaging methods, i.e. between LPS and FA. Thus, this is the first study showing that stronger pathways and higher LPS regarding the same cohort of participants and virtually the same regions of the brain both are associated with a reduced verbal lateralisation to the left hemisphere.

As anticipated, right ear advantage was detected among most participants. Kimura (2011) suggests that this is due to left hemisphere dominance for language and due to dominance of contralateral tracks over unilateral paths during dichotic listening. While a right ear input is directly transferred via contralateral tracks to the left hemisphere, a left ear input first arrives to the right hemisphere, to then be transferred to the left. This requires more time and is suggested to generate the so called right ear advantage. Our results of significant correlation between higher FA for the pSTG connection and low LI underpin Kimura's modell. This implies the interhemispheric connecting pathway determines and influences the level of language lateralisation. These findings fit with those of Westerhausen et al. (2009), who showed that an increased midsagittal cross surface through the splenium of the CC considering the same ROIs used here (HG, pSTG), is associated with higher number of correct left ear reports. Similarly, Josse et al. (2009) demonstrated using structural MRI that greater CC correlates with stronger left speech lateralisation. Unlike other similar studies, in our research FA within the entire connecting tract

was analysed rather than only within the CC or its midsaggital part. Only the FA value was considered, since mean diffusivity, AD, RD or volume of tracts are less reliable parameters. As well, a multiple-regression analysis yielded only FA and gamma synchronisation contributes significantly as predictors for language lateralisation.

Subjects with a stronger tendency to perceive syllables presented to the LE show higher mean FA values within the tracts connecting both pSTG. Subjects with lower LI have higher mean FA values within the tracts connecting both pSTGs. Accordingly, subjects with either less correct RE reports or more LE reports have higher mean FA values. In other words, LE dominance means higher FA values in WM connecting left and right auditory cortices. FA provides information about directionality and allows for the making of assumptions regarding micro structure of brain tissue. The root cause of the higher FA may be thicker isolation (myelin), higher axonal density and low axonal diameter. Except for low axonal diameter, higher FA value can be interpreted as a stronger structural connection (Koerte and Muehlmann 2014). Taking all this into consideration, it can be concluded that a stronger connection between the left and right auditory regions means higher left ear advantage (LEA). Increased interhemispheric auditory connectivity leads to a faster right to left transfer and therefore to a stronger LE perception, and therefore outweigh the direct connection from the RE to the LH, as mentioned in the introduction.

These findings were not limited to DTI findings, but are also reflected in the EEG data analysis. Gamma-band synchrony between homolog cortical structures was significantly (negatively) correlated with LI and the number of correct RE reports, and (positively) with correct LE reports. Using an LPS analysis, a significant correlation between DL performance and LPS was found. For the analysis, mean LPS in the gamma-band range (30-100 Hz) for the first 800ms after event (syllable presentation) was used. Higher LPS was found within lower LI for the connection of pSTG, yet not for the connection of HG. LPS is an indicator of functional connectivity (Pascual-Marqui 2007a). Therefore it can be concluded, that stronger auditory connectivity is found in conjunction with LE supremacy. The findings conform with earlier DTI and EEG studies (Westerhausen et al. 2006, Steinmann et al. 2014b,

2017). By simultaneous use of DTI and EEG the high over-time-resolution of EEG (milliseconds) as well as exact fine structural information of the DTI analysis (millimetres) was obtained. Both together allows for higher reliability. Yet, the combination has its limitations. Since EEG information is very fragile, each measurement was conducted separately. This has to do with the conditions within an MRI scanner (noise and strong magnetic field). All these can lead to artefacts, and even to confounding, as noise appear to have an influence on binaural perception (Dos Santos Sequeira et al. 2010). In order to reduce chances of differences between time of scan and time of EEG, both MRI and EEG had to be conducted no more than two weeks apart.

Moreover, the interhemispheric connectivity has been discussed in relation to the occurrence of AVH in schizophrenia patients: In a DTI study, Hubl et al. (2004) found higher FA values in the corresponding intercallosal midsagittal area of the tractography discussed in this thesis for patients suffering from AVH in comparison with not hallucinating schizophrenia patients. Hence, a stronger connectivity has been observed typically in schizophrenia patients with AVH. This suggests that these alterations may help to understand the origin of AVH. Mulert et al. (2011) found in an EEG study that LPS of GBO of HG correlate positively with the severity of AVH, using AVH symptom scores. Both studies suggest that better interhemispheric connection of auditory cortices might, within patients with schizophrenia, increase their chances of developing AVH as well as their severity. Until now, no such correlation for healthy individuals have been observed, and therefore one cannot speak of a higher tendency of developing schizophrenia for individuals with LE supremacy, reduced RE reports, higher LPS or higher FA between auditory cortices. There is also no study showing if such individuals, after developing schizophrenia, might be more likely to experience AVH, since DL findings for schizophrenia patients are always post-diagnosis, and therefore cannot reflect the constitution before developing the disease. It would be interesting to examine whether these parameters could be used as markers for predisposition of schizophrenia, as finding of such a marker could lead to earlier intervention and to primary prevention, which would result in better outcomes.

As pointed out in an editorial in "Nature" (2010) "A decade for psychiatric disorders", one of the main limitations of psychiatry is the late diagnosis of disorders, mostly when the conditions have already manifested themselves and are harder to control. This is different than with other disciplines of medicine where in many cases a diagnosis can be done in an early stage of the disease, or before it outbreaks (risk factors). Early diagnosis leads to early intervention and to better outcomes. Psychiatric patients should not be denied the same quality of care. Therefore extensive research in these fields is sorely lacking.

Nonetheless, FA is a far from being a perfect parameter. As mentioned above, high FA stands for high axonal density and higher isolation (myelin) but also for thinner axons. While the first two conform with stronger connectivity, it is known that thicker, and not thinner axons deliver information faster. The reason is that FA is a mathematical definition and is not defined by whether connectivity is better or not. Therefore it can only provide a limited indication of the connectivity itself. Hence, not one but two neuroimage methods, i.e. EEG analysis as well, were used in order to obtain a stronger statement. There are many ways to conduct a DTI analysis and no standardised protocol. Thus, the same results could have been produced with different methods, but could also produce adverse or no results. This is partially due to the complexity of the analysis. In many occasions, one must decide upon a threshold or method. Every time such decision had to be made the rest of the research group, as well as other researchers working with FSL were consulted, trying always to choose the most parsimonious and most reasonable method.

Finaly, this study demonstrate that the micro-architecture of individual fiber tracks connecting homolog pSTG areas as well as interhemispheric gamma-band synchrony between homolog pSTG, are both related to conscious perception of syllables, and further, that higher values within both measures reduce the common leftward language lateralisation. Concurrently, the results indicate that GBO synchronization is a better or for perception than the structural interhemispheric fibre connections as obtained by DTI. In this manner, a combination of different neuroimaging forms reveals new ways for grasping the neural associations of conscious perception.

5. Summary

The perception of speech is one of the most complex features of our brain. Models to examine anatomical structures through which auditory impulses are transferred upward to the cortex have become well-established. However, function-structure relations, their discrepancies, and their importance are the subject of current research and scientific discussion. The study presented here focuses on the language lateralisation of syllables. In particular, it examines the extent to which dichotic listening, i.e. the simultaneous perception of different auditory input to each ear, functions as an instrument to show speech lateralisation in terms of right or left ear dominance.

The results of a dichotic listening task serve in this study as an endpoint, the fractional anisotrophy as a measure of directionality, derived from DTI imaging as well as from a connectivity analysis of gamma frequency (30-100 Hz) from EEG recording. The study presented here is a multimodal study. Each method contributes to the total of the acquired information. The DTI analysis provides a high spatial resolution, while the EEG analysis provides a high temporal resolution. As a benefit, we gain higher hypothesis validity as well as the possibility to examine both methods at once.

The study, including 27 participants, has shown that a stronger interhemispheric connection correlates with lateralisation to the left ear. An association between both imaging methods could not yet be shown. The results of the study substantiate results of previous studies considering speech lateralisation. This study is, however, the first to show such correlation within a single cohort using both methods, EEG and DTI. As such, this study introduces basis for further clarification of the meaning of such structure-function interindividual differences, eventually paving the way for earlier diagnosis of psychiatric and neurologic diseases and better medical outcomes.

6. Zusammenfassung (Summary in German)

Die Wahrnehmung von Sprache gehört zu den komplexeren Vorgängen unseres Gehirns. Etablierte Modelle, welche die anatomischen Strukturen durch die auditorischen Impulse auf deren Weg zum Kortex untersuchen, genießen inzwischen breite Akzeptanz. Dagegen sind Funktion-Struktur Beziehungen und die Untersuchung deren Unterschiede sowie ihrer Bedeutung Gegenstand aktueller Forschung. Die hier vorgestellte Studie fokussiert sich auf die Sprachlateralisation von Silben. Dabei wird insbesondere untersucht, inwieweit das dichotische Hören, i.e. die gleichzeitige Wahrnehmung verschiedener Inputs in jedem Ohr, als Instrument zur Darstellung der Sprachlateralisation im Sinne einer Rechts- bzw. Linksohr Dominanz funktioniert.

Als Endpunkte fungieren in dieser Studie die Ergebnisse aus der dichotischen Höraufgabe, die fraktionelle Anisotropie als Maß für Direktionalität abgeleitet aus einer DTI-Aufnahme, sowie die Konnektivitätsanalyse bezogen auf gamma Frequenzbereich (30-100 Hz) anhand EEG-Analyse. Dabei handelt es sich um eine multimodale Studie. Jede Methode trägt zur Gesamtheit der gewonnenen Information bei: Die DTI-Analyse liefert eine hohe räumliche Auflösung, während die EEG-Analyse eine hohe zeitliche Auflösung bietet. Als Vorteil erhält man somit eine erhöhte Validität der Aussage sowie die Möglichkeit, beide Methoden gemeinsam zu betrachten.

Die Studie mit 27 Probanden hat ergeben, dass eine stärkere interhemispherische Verbindung mit einer Lateralisation zum linken Ohr korreliert. Eine Assoziation zwischen beiden bildgebenden Methoden konnte jedoch nicht gezeigt werden. Die Ergebnisse untermauern Ergebnisse früherer Studien bezüglich der Sprachlateralisierung. Diese Studie ist jedoch die erste, die diese Korrelation innerhalb einer Kohorte bezüglich beider Methoden, EEG und DTI zeigen konnte. Somit legt die Studie eine Grundlage zur weiteren Klärung der Frage nach der Bedeutung solcher anatomisch funktionalen Unterschiede und trägt eventuell bei auf dem Weg zur zukünftigen Früherkennung psychiatrischer und neurologischer Krankheiten und somit zur Erreichung besserer klinischer Ergebnisse.

7. List of Abbreviations

AD: axial diffusivity
AVH: auditory verbal hallucinations
BA: Brodmann area
BET: Brain Exctraction Tool
CC: corpus calossum
CSF: cerebrospinal fluid
CV: consonant vowel
DICOM: digital imaging and communication in medicine
DL: dichotic listening
DOF: degrees of freedom
DTI: diffusion tensor imaging
EEG: electroencephalography
FA: fractional anisotropy
FDT: FMRIB Diffusion Toolbox
fMRI: functional magnetic resonance imaging
FSL: FMRIB Software Library
GBO: Gamma-band oscillation
HG: Heschl's gyrus
LE: left ear
LEA: left ear advantage
LH: left hemisphere
LI: laterality index
LPS: lagged phase synchronisation
MD: mean diffusivity
MRI: magnetic resonance imaging
NIfTI: neuroimaging informatics technology initiative
PAC: primary auditory cortex
pSTG: posterior division of the superior temporal gyrus
RD: radial diffusivity
RE: right ear
REA: right ear advantage
RH: right hemisphere
ROI: region of interest
SAC: secondary auditory cortex
VOT: voice onset time
WM: white matter

8. References

Aboitiz F, Scheibel AB, Fisher RS, Zaidel E (1992) Fiber composition of the human corpus callosum. Brain research 598: 143–53.

Alvarez V, Rossetti A (2014) Electroencephalography and Evoked Potentials: Technical Background. In: AO Rossetti and S Laureys, editor. Clinical Neurophysiology in Disorders of Consciousness SE - 2 Springer Vienna. p. 7–23.

Bamiou D-E, Sisodiya S, Musiek FE, Luxon LM (2007) The role of the interhemispheric pathway in hearing. Brain research reviews 56: 170–82.

Behrens TEJ, Berg HJ, Jbabdi S, Rushworth MFS, Woolrich MW (2007) Probabilistic diffusion tractography with multiple fibre orientations: What can we gain? NeuroImage 34: 144–55.

Behrens TEJ, Johansen-Berg H, Woolrich MW, Smith SM, Wheeler-Kingshott CAM, Boulby PA, Barker GJ, Sillery EL, Sheehan K, Ciccarelli O, Thompson AJ, Brady JM, Matthews PM (2003a) Non-invasive mapping of connections between human thalamus and cortex using diffusion imaging. Nature neuroscience 6: 750–7.

Behrens TEJ, Woolrich MW, Jenkinson M, Johansen-Berg H, Nunes RG, Clare S, Matthews PM, Brady JM, Smith SM (2003b) Characterization and propagation of uncertainty in diffusion-weighted MR imaging. Magnetic resonance in medicine 50: 1077–88.

Berger H (1929) Über das Elektrenkephalogramm des Menschen. Archiv für Psychiatrie und Nervenkrankheiten 87: 527–570.

Le Bihan D (2003) Looking into the functional architecture of the brain with diffusion MRI. Nature Reviews Neuroscience 4: 469–480.

Boatman D (2004) Cortical bases of speech perception: Evidence from functional lesion studies. Cognition 92: 47–65.

Brancucci A, Babiloni C, Babiloni F, Galderisi S, Mucci A, Tecchio F, Zappasodi F, Pizzella V, Romani GL, Rossini PM (2004) Inhibition of auditory cortical responses to ipsilateral stimuli during dichotic listening: evidence from magnetoencephalography. The European journal of neuroscience 19: 2329–36.

Broadbent D (1954) The role of auditory localization in attention and memory span. Journal of Experimental Psychology 47: 191–196.

Carl C, Açik A, König P, Engel AK, Hipp JF (2012) The saccadic spike artifact in MEG. NeuroImage 59: 1657–1667.

Caton R (1875) The Electric Currents of the Brain. Brit Med J 2: 278-.

Collins L (1994) 3D model-based segmentation of individual brain structures from magnetic resonance imaging data.

Csicsvari J, Jamieson B, Wise KD, Buzsáki G (2003) Mechanisms of gamma oscillations in the hippocampus of the behaving rat. Neuron 37: 311–22.

Desikan RS, Ségonne F, Fischl B, Quinn BT, Dickerson BC, Blacker D, Buckner RL, Dale AM, Maguire RP, Hyman BT, Albert MS, Killiany RJ (2006) An automated labeling system for subdividing the human cerebral cortex on MRI scans into gyral based regions of interest. NeuroImage 31: 968–80.

Diesch E, Schummer V, Kramer M, Rupp A (2012) Structural changes of the corpus callosum in tinnitus. Frontiers in systems neuroscience 6: 17.

Evans AC, Marrett S, Neelin P, Collins L, Worsley K, Dai W, Milot S, Meyer E, Bub D (1992) Anatomical mapping of functional activation in stereotactic coordinate space. NeuroImage 1: 43–53.

Finger H, Bönstrup M, Cheng B, Messé A, Hilgetag C, Thomalla G, Gerloff C, König P (2016) Modeling of Large-Scale Functional Brain Networks Based on Structural Connectivity from DTI: Comparison with EEG Derived Phase Coupling Networks and Evaluation of Alternative Methods along the Modeling Path. PLoS computational biology 12: e1005025.

Henshall KR, Sergejew AA, McKay CM, Rance G, Shea TL, Hayden MJ, Innes-Brown H, Copolov DL (2012) Interhemispheric transfer time in patients with auditory hallucinations: An auditory event-related potential study. International Journal of Psychophysiology 84: 130–139.

Herzfeld H (1994) WST-Wortschatztest. Karl-Heinz Schmidt und Peter Metzler. Weinheim: Beltz Test GmbH, 1992. Diagnostica 40: 293–297.

Hickok G, Poeppel D (2007) The cortical organization of speech processing. Nature Reviews Neuroscience 8: 393–402.

Hubl D, Koenig T, Strik W, Federspiel A, Kreis R, Boesch C, Maier SE, Schroth G, Lovblad K, Dierks T (2004) Pathways that make voices: white matter changes in auditory hallucinations. Archives of general psychiatry 61: 658–68.

Hugdahl K (2003) Dichotic listening in the study of auditory laterality. In: DRJ Hugdahl K, editor. The Asymmetrical Brain Cambridge: MIT Press. p. 441–

475.

Hugdahl K, Andersson L (1986) The “forced-attention paradigm” in dichotic listening to CV-syllables: a comparison between adults and children. Cortex; a journal devoted to the study of the nervous system and behavior 22: 417–32.

Hugdahl K, Carlsson G, Uvebrant P, Lundervold AJ (1997) Dichotic-listening performance and intracarotid injections of amobarbital in children and adolescents. Preoperative and postoperative comparisons. Archives of neurology 54: 1494–500.

Hugdahl K, Westerhausen R (2010) The Two Halves of the Brain. Information Processing in the Cerebral Hemispheres edited.

Inano S, Takao H, Hayashi N, Abe O, Ohtomo K (2011) Effects of Age and Gender on White Matter Integrity. American Journal of Neuroradiology 32: 2103–2109.

Jbabdi S, Sotiropoulos SN, Savio AM, Graña M, Behrens TEJ (2012) Model-based analysis of multishell diffusion MR data for tractography: how to get over fitting problems. Magnetic resonance in medicine 68: 1846–55.

Jenkinson M, Beckmann C., Behrens TE, Woolrich MW, Smith SM (2012) FSL. NeuroImage 62: 782–90.

Jenkinson M, Pechaud M, Smith S (2005) BET2: MR-based estimation of brain, skull and scalp surfaces.

Josse G, Seghier ML, Kherif F, Price CJ (2009) Explaining Function with Anatomy : Language Lateralization and Corpus Callosum Size. Neuroscience 28: 14132–14139.

Kimura D (1961a) Cerebral dominance and the perception of verbal stimuli. Canadian Journal of Psychology/Revue canadienne de psychologie 15: 166–171.

Kimura D (1961b) Some effects of temporal-lobe damage on auditory perception. Canadian journal of psychology 15: 156–165.

Kimura D (1967) Functional Asymmetry of the Brain in Dichotic Listening. Cortex 3: 163–178.

Kimura D (2011) From ear to brain. Brain and Cognition 76: 214–217.

Koerte IK, Muehlmann M (2014) MRI in Psychiatry. C. Mulert, M. E. Shenton. Berlin, Heidelberg: Springer Berlin Heidelberg.

Lee CC, Winer JA (2008) Connections of cat auditory cortex: II. Commissural

system. The Journal of comparative neurology 507: 1901–19.

Mulert C, Kirsch V, Pascual-Marqui R, McCarley RW, Spencer KM (2011) Long-range synchrony of γ oscillations and auditory hallucination symptoms in schizophrenia. International journal of psychophysiology : official journal of the International Organization of Psychophysiology 79: 55–63.

Ocklenburg S, Schlaffke L, Hugdahl K, Westerhausen R (2014) From structure to function in the lateralized brain: How structural properties of the arcuate and uncinate fasciculus are associated with dichotic listening performance. Neuroscience Letters 580: 32–36.

Ocklenburg S, Westerhausen R, Hirnstein M, Hugdahl K (2013) Auditory hallucinations and reduced language lateralization in schizophrenia: a meta-analysis of dichotic listening studies. Journal of the International Neuropsychological Society : JINS 19: 410–8.

Oldfield RC (1971) The assessment and analysis of handedness: the Edinburgh inventory. Neuropsychologia 9: 97–113.

Oxford (2015) [Internet]. Available from: http://www.oxforddictionaries.com/de/definition/englisch/dichotic

Pape HC (2014) Physiologie. In: HC Pape, A Kurtz, and S Silbernagel, editor. Stuttgart, New York: Georg Thieme Verlag KG. p. 923–925.

Pascual-marqui RD (1999) Review of methods for solving the EEG inverse problem. International Journal of psychophysiology 1: 75–86.

Pascual-Marqui RD (2007a) Coherence and phase synchronization: generalization to pairs of multivariate time series, and removal of zero-lag contributions. .

Pascual-Marqui RD (2007b) Discrete, 3D distributed, linear imaging methods of electric neuronal activity. Part 1: exact, zero error localization. Clinical Neurophysiology 112: 845–852.

Pascual-marqui RD, Esslen M, Kochi K, Lehmann D (2002) Functional imaging with low resolution electromagnetic tomography (LORETA): review , comparisons , and new validation brain new. Japanese Journal of Clinical Neurophysiology 30: 81–94.

Pascual-Marqui RD, Michel CM, Lehmann D (1994) Low resolution electromagnetic tomography: a new method for localizing electrical activity in the brain. International Journal of Psychophysiology 18: 49–65.

Picton TW, Bentin S, Berg P, Donchin E, Hillyard SA, Johnson R, Miller GA, Ritter

W, Ruchkin DS, Rugg MD, Taylor MJ (2000) Guidelines for using human event-related potentials to study cognition: recording standards and publication criteria. Psychophysiology 37: 127–52.

Poeppel D, Emmorey K, Hickok G, Pylkkanen L (2012) Towards a New Neurobiology of Language. Journal of Neuroscience 32: 14125–14131.

Rimol LM, Eichele T, Hugdahl K (2006) The effect of voice-onset-time on dichotic listening with consonant–vowel syllables. Neuropsychologia 44: 191–196.

Salat DH, Tuch DS, Greve DN, Van Der Kouwe AJW, Hevelone ND, Zaleta AK, Rosen BR, Fischl B, Corkin S, Diana Rosas H, Dale AM (2005) Age-related alterations in white matter microstructure measured by diffusion tensor imaging. Neurobiology of Aging 26: 1215–1227.

Dos Santos Sequeira S, Specht K, Moosmann M, Westerhausen R, Hugdahl K (2010) The effects of background noise on dichotic listening to consonant-vowel syllables: An fMRI study. Laterality 15: 577–96.

Smith SM (2002) Fast robust automated brain extraction. Human Brain Mapping 17: 143–155.

Stam CJ, Nolte G, Daffertshofer A (2007) Phase lag index: Assessment of functional connectivity from multi channel EEG and MEG with diminished bias from common sources. Human Brain Mapping 28: 1178–1193.

Steinmann S, Leicht G, Ertl M, Andreou C, Polomac N, Westerhausen R, Friederici AD, Mulert C (2014a) Conscious auditory perception related to long-range synchrony of gamma oscillations. NeuroImage 100: 435–443.

Steinmann S, Leicht G, Ertl M, Andreou C, Polomac N, Westerhausen R, Friederici AD, Mulert C (2014b) Conscious auditory perception related to long-range synchrony of gamma oscillations. NeuroImage 100: 435–443.

Steinmann S, Leicht G, Mulert C (2014c) Interhemispheric auditory connectivity: structure and function related to auditory verbal hallucinations. Frontiers in human neuroscience 8: 55.

Steinmann S, Meier J, Nolte G, Engel AK, Leicht G, Mulert C (2017) The Callosal Relay Model of Interhemispheric Communication: New Evidence from Effective Connectivity Analysis. Brain Topography 1–9.

Sullivan E V., Pfefferbaum A (2006) Diffusion tensor imaging and aging. Neuroscience and Biobehavioral Reviews 30: 749–761.

Trepel M (2015) Neuroanatomie : Struktur und Funktion. München: Elsevier,

Urban & Fischer.

Vecchio F, Miraglia F, Curcio G, Altavilla R, Scrascia F, Giambattistelli F, Quattrocchi CC, Bramanti P, Vernieri F, Rossini PM (2015) Cortical brain connectivity evaluated by graph theory in dementia: a correlation study between functional and structural data. Journal of Alzheimer's disease : JAD 45: 745–56.

Westerhausen R, Grüner R, Specht K, Hugdahl K (2009) Functional relevance of interindividual differences in temporal lobe callosal pathways: a DTI tractography study. Cerebral cortex (New York, N.Y. : 1991) 19: 1322–9.

Westerhausen R, Woerner W, Kreuder F, Schweiger E, Hugdahl K, Wittling W (2006) The role of the corpus callosum in dichotic listening: a combined morphological and diffusion tensor imaging study. Neuropsychology 20: 272–279.

Yuval-Greenberg S, Tomer O, Keren AS, Nelken I, Deouell LY (2008) Transient Induced Gamma-Band Response in EEG as a Manifestation of Miniature Saccades. Neuron 58: 429–441.

Zschocke S, Hansen H-C (2012) Klinische Elektroenzephalographie. Berlin, Heidelberg: Springer Berlin Heidelberg.

(2010) A decade for psychiatric disorders. Nature 463: 9–9.

9. Acknowledgements

I would like to thank all of those who helped me on my way towards successfully completing this doctoral thesis.

First of all, I want to express my gratitude to my supervisor Prof. Dr. Christoph Mulert, the head of the Psychiatry Neuroimaging Branch of the University Medical Center Hamburg-Eppendorf, Department of Psychiatry and Psychotherapy during the time of my project. I want to thank him for continuous supervision and for introducing me to the very fascinating field of neuroimaging.

Furthermore, I would like to thank Prof. Dr. Jürgen Gallinat, the director of the Department of Psychiatry and Psychotherapy of the University Medial Center Hamburg-Eppendorf, for giving me the opportunity to work as a doctoral student. I want to thank him for giving me access to the required instrumentation necessary to perform this project.

During my project, the MRI scanner turned out to be the most important device. Therefore, I would like to thank the MRI team for allowing me to use their device, for supporting me and for helping me when something did not work out as expected.

A very special gratitude goes to my dearest Dr. rer. nat. Saskia S. Steinmann who has been my closest advisor and partner during my work. I appreciated her always having an open door for me.

I am very grateful to Dr. med. Bastian Cheng, without whom the entire MRI and DTI analysis, the most important part of this research, would not have been possible. Merely owing to his mentoring and attention I can now conduct an entire DTI analysis, from DICOM files to tractography and run statistics on it by myself.

To all test persons of this study, who have let me literally into their brains: I would like to thank all of you from the bottom of my heart. You are the very basis for this study.

In addition, a thank you to all members of the department who have helped with this study: Inessa Braun, Dr. med. Gregor Leicht, Dr. med. Stjepan Curic, Dr. med. Jonas Rauh, Stephanie Thiebes, Jan Meier, Sebastian Vauth and Lisa Valerie Bitzan. Thank you for all fruitful discussions - work related and non-work related. I had a great time in the department.

And finally, last but by no means least, I am grateful to my parents Amalia and Gabriel, who have brought me up to become who I am.

Entfällt aus datenschutzrechtlichen Gründen